Chapter 6
Self-gravitating Bose-Einstein Condensates

Pierre-Henri Chavanis

Abstract Bose-Einstein condensates play a major role in condensed matter physics. Recently, it has been suggested that they could play an important role in astrophysics also. Indeed, dark matter halos could be gigantic quantum objects made of Bose-Einstein condensates. The pressure arising from the Heisenberg uncertainty principle or from the repulsive scattering of the bosons could stabilize dark matter halos against gravitational collapse and lead to smooth core densities instead of cuspy density profiles in agreement with observations. In order to reproduce the scales of dark matter halos, the mass of the bosons may range from $10^{-24}\,\mathrm{eV/c^2}$ to a few $\mathrm{eV/c^2}$ depending whether they interact or not. At the scale of galaxies, Newtonian gravity can be used so the evolution of the wave function is governed by the Gross-Pitaevskii-Poisson system. Self-gravitating Bose-Einstein condensates have also been proposed to describe boson stars. For these compact objects, one must use general relativity and couple the Klein-Gordon equation to the Einstein field equations. In that context, it has been proposed that neutron stars could be Bose-Einstein condensate stars due to their superfluid core. Indeed, the neutrons could form Cooper pairs and behave as bosons. In that case, the maximum mass of the neutron stars depends on the scattering length of the bosons and can be as large as $2M_\odot$. This could explain recent observations of neutron stars with a mass much larger than the Oppenheimer-Volkoff limit of $0.7M_\odot$ obtained by assuming that neutron stars are ideal fermion stars. Self-gravitating Bose-Einstein condensates may also find applications in the physics of black holes. For example, when the scattering length of the bosons is negative, a Newtonian self-gravitating Bose-Einstein condensate becomes unstable above a critical mass and undergoes a gravitational collapse leading ultimately to a singularity. On the other hand, stable boson stars with a positive scattering length could mimic supermassive black holes that reside at the center of galaxies. Finally, it has been proposed that microscopic quantum black holes could be Bose-Einstein condensates of gravitons. This contribution discusses fundamental aspects of the physics of self-gravitating Bose-Einstein condensates

P.-H. Chavanis (✉)
Laboratoire de Physique Théorique (IRSAMC), CNRS and UPS,
Université de Toulouse, Toulouse, France
e-mail: chavanis@irsamc.ups-tlse.fr

X. Calmet (ed.), *Quantum Aspects of Black Holes*,
Fundamental Theories of Physics 178, DOI 10.1007/978-3-319-10852-0_6

and considers recent applications in astrophysics, cosmology and black hole physics with promising perspectives.

Keywords Bose-Einstein condensates · Self-gravitating systems · Dark matter halos · Quantum black holes

6.1 Introduction

According to contemporary cosmology, the universe is made of about 70 % dark energy, 25 % dark matter, and 5 % baryonic (visible) matter [1]. Thus, the overwhelming preponderance of matter and energy in the universe is believed to be dark, i.e. unobservable by telescopes. The dark energy is responsible for the accelerated expansion of the universe. Its origin is mysterious and presumably related to the cosmological constant or to some form of exotic fluid with negative pressure such as the Chaplygin gas [2]. On the other hand, dark matter is necessary to account for the observed flat rotation curves of galaxies [3]. Its nature is one of the most important puzzles in particle physics and cosmology. Many candidates for dark matter have been proposed, the most popular ones being the axions and the weakly interacting massive particles (WIMPs) [4].

Dark matter is usually modeled as a cold classical collisionless gas with vanishing pressure. In the cold dark matter (ΛCDM) model, primordial density fluctuations are generated during the inflation and become the seeds of the bottom-up structure formation model. The ΛCDM model successfully describes the accelerated expansion of the universe, the temperature fluctuations of the cosmic microwave background (CMB), and the large-scale structures of the universe [5]. However, it seems to encounter many problems at the scale of galactic or sub-galactic structures. Indeed, ΛCDM simulations [6] lead to r^{-1} cuspy density profiles at galactic centers (in the scales of the order of 1 kpc and smaller) while most rotation curves indicate a smooth core density [7]. In addition, the predicted number of satellite galaxies around each galactic halo is far beyond what we see around the Milky Way [8].

These problems might be solved, without altering the virtues of the ΛCDM model, if the dark matter is composed of Bose-Einstein condensates (BECs) [9]. The wave properties of the dark matter may stabilize the system against gravitational collapse providing halo cores instead of cuspy profiles. The resulting coherent configuration may be understood as the ground state of some gigantic bosonic atom where the boson particles are condensed in a single macroscopic quantum state $\psi(\mathbf{r})$. In these models, the formation of dark matter structures at small scales is suppressed by quantum mechanics. This property could alleviate the problems of the ΛCDM model such as the cusp problem and the missing satellite problem.

At the scale of galaxies, the Newtonian approximation is very good so the evolution of the wave function $\psi(\mathbf{r}, t)$ is governed by the Gross-Pitaevskii-Poisson (GPP) system. Using the Madelung [10] transformation, the Gross-Pitaevskii (GP) equation

[11–14] turns out to be equivalent to hydrodynamic (Euler) equations involving an isotropic pressure due to short-range interactions (scattering) and an anisotropic quantum pressure arising from the Heisenberg uncertainty principle. At large scales, quantum effects are negligible and one recovers the classical hydrodynamic equations of the ΛCDM model which are remarkably successful in explaining the large-scale structure of the universe. At small scales, gravitational collapse is prevented by the repulsive scattering or by the uncertainty principle. Quantum mechanics may therefore be a way to solve the problems of the ΛCDM model.

The possibility that dark matter could be in the form of BECs has a long history (see a short review in [15, 16]). In some works [17–34], it is assumed that the bosons have no self-interaction. In that case, gravitational collapse is prevented by the Heisenberg uncertainty principle which is equivalent to a quantum pressure. This leads to a mass-radius relation $MR = 9.95\,\hbar^2/\mathrm{Gm}^2$. In order to account for the mass and size of dark matter halos, the mass of the bosons must be extremely small, of the order of $m \sim 10^{-24}\,\mathrm{eV}/c^2$. Ultralight scalar fields like axions may have such small masses (multidimensional string theories predict the existence of bosonic particles down to masses of the order of $m \sim 10^{-33}\,\mathrm{eV/c}^2$). This corresponds to "fuzzy cold dark matter" [23]. In other works [35–48], it is assumed that the bosons have a repulsive self-interaction measured by the scattering length $a > 0$. In that case, gravitational collapse is prevented by the pressure arising from the scattering. In the Thomas-Fermi (TF) approximation which amounts to neglecting the quantum pressure, the resulting structure is equivalent to a polytrope of index $n = 1$. Its radius is given by $R = \pi(a\hbar^2/Gm^3)^{1/2}$, independent on its mass M. For $a \sim 10^6$ fm, corresponding to the values of the scattering length observed in terrestrial BEC experiments [49], this gives a boson mass $m \sim 1\,\mathrm{eV/c}^2$ much larger than the mass $m \sim 10^{-24}\,\mathrm{eV}/c^2$ required in the absence of self-interaction. This may be more realistic from a particle physics point of view. The general mass-radius relation of self-gravitating BECs at $T = 0$ with arbitrary scattering length, connecting the non-interacting limit ($a = 0$) to the TF limit ($GM^2\,ma/\hbar^2 \gg 1$), has been determined analytically and numerically in [15, 16].

Since atoms like ^{7}Li have negative scattering lengths in terrestrial BEC experiments [49], it may be relevant to consider the possibility of self-gravitating BECs with attractive self-interaction ($a < 0$). In that case, there exist a maximum mass $M_{\max} = 1.01\hbar/\sqrt{|a|Gm} = 5.07M_P/\sqrt{|\lambda|}$, where $\lambda = 8\pi amc/\hbar$ is the self-interaction constant and $M_P = (\hbar c/G)^{1/2}$ is the Planck mass, above which the BEC collapses [15, 16]. In most applications, this mass is extremely small (when $|\lambda| \sim 1$ it is of the order of the Planck mass $M_P = 2.18 \times 10^{-8}$ kg!) so that the collapse of the BEC is very easily realized in the presence of attractive self-interactions. This may lead to the formation of supermassive black holes at the center of galaxies. On the other hand, when the BEC hypothesis is applied in a cosmological context, an attractive self-interaction can enhance the Jeans instability and accelerate the formation of structures in the universe [50].

Self-gravitating BECs have also been proposed to describe boson stars [51–73]. For these compact objects, we must use general relativity and couple the

Klein-Gordon equation to the Einstein field equations. Initially, the study of boson stars was motivated by the axion field, a pseudo-Nambu-Goldstone boson of the Peccei-Quinn phase transition that was proposed as a possible solution to the strong CP problem in QCD. In the early works of Kaup [51] and Ruffini and Bonazzola [52], it was assumed that the bosons have no self-interaction. This leads to a maximum mass of boson stars equal to $M_{Kaup}=0.633M_P^2/m$. Above that mass no equilibrium configuration exists. In that case, the system collapses to a black hole. This maximum mass is much smaller than the maximum mass $M_{OV}=0.376M_P^3/m^2$ of fermion stars determined by Oppenheimer and Volkoff [74] in general relativity. They differ by a factor $m/M_P\ll 1$. This is because boson stars are stopped from collapsing by Heisenberg's uncertainty principle while for fermion stars gravitational collapse is avoided by Pauli's exclusion principle. For $m\sim 1\,\mathrm{GeV}/c^2$, corresponding to the typical mass of the neutrons, the Kaup mass $M_{Kaup}\sim 10^{-19}M_\odot$ is very small while $M_{OV}\sim 1M_\odot$. This describes mini boson stars like axion black holes. The mass of these mini boson stars may be too small to be astrophysically relevant. They could play a role, however, if they exist in the universe in abundance [53] or if the axion mass is extraordinary small leading to macroscopic objects with a mass M_{Kaup} comparable to the mass of the sun (or even larger) [71]. For example, axionic boson stars could account for the mass of MACHOs (between 0.3 and $0.8M_\odot$) if the axions have a mass $m\sim 10^{-10}\,\mathrm{eV}/c^2$ [68]. It has also been proposed that stable boson stars with a boson mass $m\sim 10^{-17}\,\mathrm{eV}/c^2$ could mimic supermassive black holes ($M\sim 10^6M_\odot$, $R\sim 10^7\,\mathrm{km}$) that reside at the center of galaxies [69, 72]. On the other hand, Colpi et al. [56] assumed that the bosons have a repulsive self-interaction. In the TF approximation, this leads to a maximum mass $M_{\max}=0.0612\,\sqrt{\lambda}M_P^3/m^2$ which, for $\lambda\sim 1$, is of the order of the maximum mass of fermion stars $M_{OV}=0.376M_P^3/m^2$. The self-interaction has the same effect on the bosons as the exclusion principle on the fermions. It plays the role of an interparticle repulsion (for $\lambda>0$) that dominates over uncertainty pressure and prevents catastrophic gravitational collapse. Therefore, for $m\sim 1\,\mathrm{GeV}/c^2$ and $\lambda\sim 1$, this leads to a maximum mass of the order of the solar mass $M_\odot$, similar to the mass of neutron stars, which is much larger than the maximum mass $M_{Kaup}\sim 10^{-19}M_\odot$ obtained in the absence of self-interaction (an interpolation formula giving the maximum mass for any value of the self-interaction constant λ is given in [15]). Therefore, self-interaction can significantly change the physical dimensions of boson stars, making them much more astrophysically interesting. For example, stellar mass boson stars could constitute a part of dark matter [56, 68]. On the other hand, Chavanis and Harko [73] have proposed that, due to the superfluid properties of the core of neutron stars, the neutrons (fermions) could form Cooper pairs and behave as bosons of mass $2m_n$, where $m_n=0.940\,\mathrm{GeV/c^2}$ is the mass of the neutrons. Therefore, neutron stars could actually be BEC stars! Since the maximum mass of BEC stars $M_{\max}=0.0612\,\sqrt{\lambda}M_P^3/m^2=0.307\hbar c^2\sqrt{a}/(Gm)^{3/2}$ depends on the self-interaction constant λ (or scattering length a), this allows to overcome the (fixed) maximum mass of neutron stars $M_{OV}=0.376M_P^3/m^2=0.7M_\odot$ determined by Oppenheimer and Volkoff [74] by modeling a neutron star as an ideal gas of fermions of mass m_n. By taking a scattering length of the order of 10–20 fm, we obtain a maximum mass of the order of $2M_\odot$ [73]. This could account for the

recently observed neutron stars with masses in the range of 2–2.4$M_\odot$ much larger than the Oppenheimer-Volkoff limit. For $M > M_{\rm max}$, nothing prevents the gravitational collapse of the star which becomes a black hole. On the other hand, for a boson mass of the order of $m \sim 1\,{\rm MeV/c^2}$ and a self-interaction constant $\lambda \sim 1$ we get $M_{\rm max} \sim 10^6 M_\odot$ and $R_{\rm min} \sim 10^7$ km. These parameters are reminiscent of supermassive black holes in active galactic nuclei, so that stable self-interacting boson stars with $m \sim 1\,{\rm MeV/c^2}$ could be an alternative to black holes at the center of galaxies [67]. Finally, it has been proposed recently that microscopic quantum black holes could be BECs of gravitons stuck at a critical point [75, 76]. We will show that these results can be understood easily in terms of the Kaup mass and Kaup radius.

This contribution is organized as follows. In Sect. 6.2 we provide general results concerning the GPP system describing Newtonian self-gravitating BECs. We specifically consider the non-interacting limit and the TF limit. In Sect. 6.3, we obtain an analytical approximate expression of the mass-radius relation of Newtonian self-gravitating BECs with positive or negative scattering length by using a Gaussian ansatz for the wave function and developing a simple mechanical analogy. In Sect. 6.4, we consider astrophysical applications of Newtonian self-gravitating BECs to dark matter halos. Finally, in Sect. 6.5, we consider astrophysical applications of general relativistic BECs to neutron stars, dark matter stars, supermassive black holes, and microscopic quantum black holes.

6.2 Self-gravitating Bose-Einstein Condensates

6.2.1 The Gross-Pitaevskii-Poisson System

We consider a system of N bosons with mass m in interaction. At $T = 0$ all the bosons condense into the same quantum ground state and the system is described by one order parameter $\psi({\bf r}, t)$ called the condensate wave function.[1] In the mean-field approximation, this gas of interacting BECs is governed by the GP equation [11–14]:

$$i\hbar\frac{\partial\psi}{\partial t}({\bf r}, t) = -\frac{\hbar^2}{2m}\Delta\psi({\bf r}, t) + m\Phi_{tot}({\bf r}, t)\psi({\bf r}, t), \tag{6.1}$$

$$\Phi_{tot}({\bf r}, t) = \int \rho({\bf r}', t)u(|{\bf r} - {\bf r}'|)\, d{\bf r}', \tag{6.2}$$

$$\rho({\bf r}, t) = Nm|\psi({\bf r}, t)|^2, \quad \int |\psi({\bf r}, t)|^2\, d{\bf r} = 1. \tag{6.3}$$

[1] The condensation of the bosons takes place when their thermal (de Broglie) wavelength $\lambda_T = (2\pi\hbar^2/mk_BT)^{1/2}$ exceeds their mean separation $l = n^{-1/3}$ (n is the number density of the bosons). This leads to the inequality $n\lambda_T^3 > 1$ or $T < T_c$ where $T_c = 2\pi\hbar^2 n^{2/3}/mk_B$ is the critical condensation temperature (up to a numerical proportionality factor).

Equation (6.3) is the normalization condition, Eq. (6.3) gives the density of the BECs, Eq. (6.2) determines the associated potential, and Eq. (6.1) determines the evolution of the wave function. We assume that the potential of interaction can be written as $u = u_{LR} + u_{SR}$ where u_{LR} refers to long-range interactions and u_{SR} to short-range interactions. For self-gravitating BECs in the Newtonian approximation, the long-range potential of interaction is given by $u_{LR} = -G/|\mathbf{r} - \mathbf{r}'|$ where G is the constant of gravity. We assume that the short-range interaction corresponds to binary collisions that can be modeled by the effective potential $u_{SR} = g\delta(\mathbf{r} - \mathbf{r}')$ where the coupling constant (or pseudo-potential) g is related to the s-wave scattering length a through $g = 4\pi a\hbar^2/m^3$ [49]. For the sake of generality, we allow a to be positive or negative ($a > 0$ corresponds to a short-range repulsion and $a < 0$ corresponds to a short-range attraction). Under these conditions, the total potential can be written as $\Phi_{tot} = \Phi + h(\rho)$ where $\Phi(\mathbf{r}, t)$ is the gravitational potential that is the solution of the Poisson equation $\Delta\Phi = 4\pi G\rho$ and $h(\rho) = g\rho = gNm|\psi|^2$ is an effective potential modeling short-range interactions. Regrouping these results, we obtain the GPP system

$$i\hbar\frac{\partial\psi}{\partial t} = -\frac{\hbar^2}{2m}\Delta\psi + m\Phi\psi + N\frac{4\pi a\hbar^2}{m}|\psi|^2\psi, \tag{6.4}$$

$$\Delta\Phi = 4\pi GNm|\psi|^2. \tag{6.5}$$

6.2.2 Madelung Transformation

We use the Madelung [10] transformation to rewrite the GP equation (6.4) in the form of hydrodynamic equations. We write the wavefunction as

$$\psi(\mathbf{r}, t) = A(\mathbf{r}, t)e^{iS(\mathbf{r},t)/\hbar}, \tag{6.6}$$

where $A(\mathbf{r}, t)$ and $S(\mathbf{r}, t)$ are real functions. We clearly have $A = \sqrt{|\psi|^2}$ and $S = (\hbar/2i)\ln(\psi/\psi^*)$. Following Madelung, we introduce the density and the velocity fields

$$\rho = NmA^2 = Nm|\psi|^2, \quad \mathbf{u} = \frac{1}{m}\nabla S. \tag{6.7}$$

The flow is irrotational since $\nabla \times \mathbf{u} = \mathbf{0}$. Substituting Eq. (6.6) in Eq. (6.4) and separating real and imaginary parts, we obtain

$$\frac{\partial\rho}{\partial t} + \nabla\cdot(\rho\mathbf{u}) = 0, \tag{6.8}$$

$$\frac{\partial S}{\partial t} + \frac{1}{2m}(\nabla S)^2 + m\Phi + \frac{4\pi a\hbar^2}{m^2}\rho + Q = 0, \tag{6.9}$$

where

$$Q=-\frac{\hbar^2}{2m}\frac{\Delta\sqrt{\rho}}{\sqrt{\rho}}=-\frac{\hbar^2}{4m}\left[\frac{\Delta\rho}{\rho}-\frac{1}{2}\frac{(\nabla\rho)^2}{\rho^2}\right] \tag{6.10}$$

is the quantum potential. The first equation is similar to the equation of continuity in hydrodynamics. It accounts for the conservation of mass $M=\int\rho\,d\mathbf{r}$. The second equation has a form similar to the classical Hamilton-Jacobi equation with an additional quantum term. It can also be interpreted as a generalized Bernouilli equation for a potential flow. Taking the gradient of Eq. (6.9), and using the well-known identity $(\mathbf{u}\cdot\nabla)\mathbf{u}=\nabla(\mathbf{u}^2/2)-\mathbf{u}\times(\nabla\times\mathbf{u})$ which reduces to $(\mathbf{u}\cdot\nabla)\mathbf{u}=\nabla(\mathbf{u}^2/2)$ for an irrotational flow, we obtain an equation similar to the Euler equation

$$\frac{\partial\mathbf{u}}{\partial t}+(\mathbf{u}\cdot\nabla)\mathbf{u}=-\frac{1}{\rho}\nabla p-\nabla\Phi-\frac{1}{m}\nabla Q \tag{6.11}$$

with a quantum potential Q and a pressure

$$p=\frac{2\pi a\hbar^2}{m^3}\rho^2 \tag{6.12}$$

corresponding to a polytropic equation of state $p=K\rho^{1+1/n}$ with a polytropic constant $K=2\pi a\hbar^2/m^3$ and a polytropic index $n=1$ (i.e. $\gamma=1+1/n=2$). Using the equation of continuity (6.8), we can rewrite Eq. (6.11) as

$$\frac{\partial}{\partial t}(\rho\mathbf{u})+\nabla(\rho\mathbf{u}\otimes\mathbf{u})=-\nabla p-\rho\nabla\Phi-\frac{\rho}{m}\nabla Q. \tag{6.13}$$

In conclusion, the GPP system is equivalent to the hydrodynamic equations

$$\frac{\partial\rho}{\partial t}+\nabla\cdot(\rho\mathbf{u})=0, \tag{6.14}$$

$$\frac{\partial\mathbf{u}}{\partial t}+(\mathbf{u}\cdot\nabla)\mathbf{u}=-\frac{1}{\rho}\nabla p-\nabla\Phi-\frac{1}{m}\nabla Q, \tag{6.15}$$

$$\Delta\Phi=4\pi G\rho. \tag{6.16}$$

We shall refer to these equations as the quantum Euler-Poisson system. When the quantum potential can be neglected, we obtain the classical Euler-Poisson system. The quantum potential (6.10) first appeared in the work of Madelung [10] and was rediscovered by Bohm [77] (it is sometimes called "the Bohm potential"). We note the identity $-(1/m)\nabla Q\equiv-(1/\rho)\partial_j P_{ij}$ where P_{ij} is the quantum pressure tensor

$$P_{ij}=-\frac{\hbar^2}{4m^2}\rho\,\partial_i\partial_j\ln\rho\quad\text{or}\quad P_{ij}=\frac{\hbar^2}{4m^2}\left(\frac{1}{\rho}\partial_i\rho\partial_j\rho-\delta_{ij}\Delta\rho\right). \tag{6.17}$$

These identities show that the quantum potential Q is equivalent to an anisotropic pressure P_{ij}. By contrast, the potential of short-range interaction $h(\rho)$ is equivalent to an isotropic pressure $p(\rho)$. This pressure is different from a thermodynamic pressure. In particular, it is negative for an attractive self-interaction ($a < 0$).

6.2.3 Time-Independent GP Equation

If we consider a wavefunction of the form

$$\psi(\mathbf{r}, t) = A(\mathbf{r})e^{-iEt/\hbar}, \tag{6.18}$$

we obtain the time-independent GP equation

$$-\frac{\hbar^2}{2m}\Delta\phi(\mathbf{r}) + m\Phi(\mathbf{r})\phi(\mathbf{r}) + N\frac{4\pi a\hbar^2}{m}\phi(\mathbf{r})^3 = E\phi(\mathbf{r}), \tag{6.19}$$

where $\phi(\mathbf{r}) \equiv A(\mathbf{r})$ is real and $\rho(\mathbf{r}) = Nm\phi^2(\mathbf{r})$. Dividing Eq. (6.19) by $\phi(\mathbf{r})$, we get

$$m\Phi + \frac{4\pi a\hbar^2}{m^2}\rho - \frac{\hbar^2}{2m}\frac{\Delta\sqrt{\rho}}{\sqrt{\rho}} = E. \tag{6.20}$$

This relation can also be derived from the quantum Hamilton-Jacobi equation (6.9) by setting $S = -Et$. Combined with the Poisson equation (6.5) or (6.16), we obtain an eigenvalue equation for the wave function $\phi(\mathbf{r})$, or for the density $\rho(\mathbf{r})$, where the eigenvalue is the eigenenergy E. In the following, we shall be interested by the fundamental eigenmode corresponding to the smallest value of E. For this mode, the wave function $\phi(r)$ is spherically symmetric and has no node so that the density profile decreases monotonically with the distance. The "excited" modes (presenting nodes or oscillations) are unstable and decay to the ground state.

6.2.4 Hydrostatic Equilibrium

The time-independent solution (6.20) can also be obtained from the quantum Euler equation since it is equivalent to the GP equation. The steady state of the quantum Euler equation (6.15), obtained by setting $\partial_t = 0$ and $\mathbf{u} = \mathbf{0}$, satisfies

$$\nabla p + \rho\nabla\Phi - \frac{\hbar^2\rho}{2m^2}\nabla\left(\frac{\Delta\sqrt{\rho}}{\sqrt{\rho}}\right) = \mathbf{0}. \tag{6.21}$$

This generalizes the usual condition of hydrostatic equilibrium by incorporating the contribution of the quantum potential. Equation (6.21) describes the balance between the gravitational attraction, the repulsion due to the quantum potential, and the repulsion (for $a > 0$) or the attraction (for $a < 0$) due to the short-range interaction (scattering). This equation is equivalent to Eq. (6.20). Indeed, integrating Eq. (6.21) using Eq. (6.12), we obtain Eq. (6.20) where the eigenenergy E appears as a constant of integration. On the other hand, combining Eq. (6.21) with the Poisson equation (6.16), we obtain the fundamental equation of hydrostatic equilibrium for self-gravitating systems including the quantum potential

$$-\nabla\cdot\left(\frac{\nabla p}{\rho}\right)+\frac{\hbar^2}{2m^2}\Delta\left(\frac{\Delta\sqrt{\rho}}{\sqrt{\rho}}\right)=4\pi G\rho. \tag{6.22}$$

This equation is actually valid for an arbitrary equation of state $p(\rho)$ [15]. For the equation of state (6.12), it becomes

$$-\frac{4\pi a\hbar^2}{m^3}\Delta\rho+\frac{\hbar^2}{2m^2}\Delta\left(\frac{\Delta\sqrt{\rho}}{\sqrt{\rho}}\right)=4\pi G\rho. \tag{6.23}$$

Assuming spherical symmetry, this equation can be solved numerically [16] to yield the density profile $\rho(r)$ and the mass-radius relation for any value of the scattering length a. There are two important limits that we discuss in the following.

6.2.5 The Non-interacting Case

In the non-interacting case ($a = p = 0$), the condition of hydrostatic equilibrium (6.21) reduces to

$$\rho\nabla\Phi-\frac{\hbar^2\rho}{2m^2}\nabla\left(\frac{\Delta\sqrt{\rho}}{\sqrt{\rho}}\right)=\mathbf{0}. \tag{6.24}$$

This corresponds to the balance between the gravitational attraction and the repulsion due to the quantum pressure arising from the Heisenberg uncertainty principle. Combined with the Poisson equation (6.16), we obtain the differential equation

$$\frac{\hbar^2}{2m^2}\Delta\left(\frac{\Delta\sqrt{\rho}}{\sqrt{\rho}}\right)=4\pi G\rho. \tag{6.25}$$

This equation has been solved numerically in [16, 18, 52]. The density decays smoothly to infinity. The radius of the configuration containing 99 % of the mass is

$$R_{99} = 9.95\frac{\hbar^2}{GMm^2}. \tag{6.26}$$

We note that $R_{99} = 9.95a_B/N$ where $a_B = \hbar^2/Gm^3$ is the gravitational Bohr radius.

6.2.6 The Thomas-Fermi Approximation

The TF approximation amounts to neglecting the quantum potential in Eq. (6.21). In that case, Eq. (6.21) reduces to the usual condition of hydrostatic equilibrium

$$\nabla p + \rho\nabla\Phi = \mathbf{0}. \tag{6.27}$$

This corresponds to the balance between the gravitational attraction and the repulsion due to the short-range interaction (when $a > 0$). Combined with the Poisson equation (6.16), we obtain the fundamental equation of hydrostatic equilibrium for self-gravitating systems

$$-\nabla\cdot\left(\frac{\nabla p}{\rho}\right) = 4\pi G\rho. \tag{6.28}$$

For the equation of state (6.12), it can be rewritten as

$$\Delta\rho + \frac{Gm^3}{a\hbar^2}\rho = 0. \tag{6.29}$$

This equation, which is equivalent to the Lane-Emden equation for a polytrope of index $n = 1$, can be solved analytically [78]. The density profile is given by the formula

$$\rho(r) = \frac{\rho_0 R}{\pi r}\sin\left(\frac{\pi r}{R}\right), \tag{6.30}$$

where ρ_0 is the central density and

$$R = \pi\left(\frac{a\hbar^2}{Gm^3}\right)^{1/2} \tag{6.31}$$

is the radius of the configuration at which the density vanishes (the density has a compact support) [15, 35, 37, 39, 40]. The radius of a polytrope $n = 1$ is independent on its mass M [78]. The radius containing 99 % of the mass is given by $R_{99} = 0.954R$. The central density is determined by the mass according to $\rho_0 = \pi M/4R^3 = (M/4\pi^2)\left(Gm^3/a\hbar^2\right)^{3/2}$. Finally, it can be shown that polytropes with index $\gamma > 4/3$, including the polytrope $\gamma = 2$ ($n = 1$) corresponding to Eq. (6.12), are nonlinearly dynamically stable with respect to the classical Euler-Poisson system. Therefore, the density profile (6.30) valid in the TF limit is dynamically stable.

6.2.7 Validity of the Thomas-Fermi Approximation

In the absence of short-range interaction, the structure of the self-gravitating BEC results from the balance between the gravitational attraction and the quantum pressure arising from the Heisenberg uncertainty principle. Using dimensional analysis in Eq. (6.23), i.e. writing $\hbar^2/m^2R^4 \sim GM/R^3$, we obtain the length-scale

$$R_Q = \frac{\hbar^2}{GMm^2} \tag{6.32}$$

which gives the typical size of a self-gravitating BEC with mass M without short-range interaction ($a = 0$).

In the TF approximation, in which the quantum potential is negligible, the structure of the self-gravitating BEC results from the balance between the gravitational attraction and the short-range repulsion due to scattering (when $a > 0$). Using dimensional analysis in Eq. (6.23), i.e. writing $(a\hbar^2/m^3R^2)(M/R^3) \sim GM/R^3$, we obtain the length-scale

$$R_a = \left(\frac{a\hbar^2}{Gm^3}\right)^{1/2} = \left(\frac{\lambda\hbar^3}{8\pi Gm^4c}\right)^{1/2} = \sqrt{\frac{\lambda}{8\pi}}\frac{M_P}{m}\lambda_c \tag{6.33}$$

which gives the typical size of a self-gravitating BEC with scattering length $a > 0$ in the TF approximation (we have introduced the self-interaction constant λ and the Compton wavelength λ_c defined in Appendix 6.7).

Considering Eq. (6.23) again, the quantum pressure and the pressure arising from the short-range interaction become comparable when $(|a|\hbar^2/m^3R^2)(M/R^3) \sim \hbar^2/m^2R^4$, i.e. $N|a|/R \sim 1$. Estimating R by Eq. (6.32) or (6.33), this condition can be rewritten $\chi \sim 1$ where we have introduced the important dimensionless parameter

$$\chi \equiv \frac{GM^2m|a|}{\hbar^2} = \frac{|\lambda|}{8\pi}\frac{GM^2}{\hbar c} = \frac{|\lambda|}{8\pi}\frac{M^2}{M_P^2}. \tag{6.34}$$

When $\chi \gg 1$, we are in the TF limit in which the quantum potential is negligible. This corresponds to $R_a \gg R_Q$. In that case, the equilibrium state results from the balance between gravitational attraction and repulsive scattering (when $a > 0$). Alternatively, when $\chi \ll 1$, we are in the non-interacting limit in which scattering is negligible. This corresponds to $R_a \ll R_Q$. In that case, the equilibrium state results from the balance between gravitational attraction and quantum pressure. The transition between these two regimes occurs for $\chi \sim 1$. For a given value of the scattering length a, the TF approximation is valid when $M \gg M_a$ where

$$M_a = \frac{\hbar}{\sqrt{Gm|a|}} = \left(\frac{8\pi\hbar c}{G|\lambda|}\right)^{1/2} = \frac{M_P}{\sqrt{\frac{|\lambda|}{8\pi}}}, \tag{6.35}$$

and the non-interacting approximation is valid when $M \ll M_a$. For a given value of the mass M, the TF approximation is valid when

$$|a| \gg \frac{\hbar^2}{GM^2m}, \quad m \gg \frac{\hbar^2}{GM^2|a|}, \quad \frac{|\lambda|}{8\pi} \gg \frac{\hbar c}{GM^2} = \frac{M_P^2}{M^2}. \tag{6.36}$$

Remark With the mass M_a and the radius R_a we can form a density $\rho_a = M_a/R_a^3 = Gm^4/a^2\hbar^2$, an energy $E_a = GM_a^2/R_a = \hbar(Gm)^{1/2}/|a|^{3/2}$, and a time $t_a = 1/\sqrt{G\rho_a} = |a|\hbar/Gm^2$. In the figures we shall use dimensionless variables normalized by M_a, R_a, ρ_a, E_a, and t_a (for given a). This is equivalent to taking $\hbar = G = m = |a| = 1$ in the dimensional equations of the text.

6.2.8 The Total Energy

The total energy associated with the GPP system (6.4)–(6.5), or equivalently with the quantum Euler-Poisson system (6.14)–(6.16), can be written as

$$E_{tot} = \Theta_c + \Theta_Q + U + W. \tag{6.37}$$

The first two terms correspond to the total kinetic energy $\Theta = \frac{N\hbar^2}{2m}\int |\nabla\psi|^2\, d\mathbf{r}$. Using the Madelung transformation, it can be decomposed into the "classical" kinetic energy Θ_c and the "quantum" kinetic energy Θ_Q defined by

$$\Theta_c = \int \rho \frac{\mathbf{u}^2}{2}\, d\mathbf{r}, \quad \Theta_Q = \frac{1}{m}\int \rho Q\, d\mathbf{r}. \tag{6.38}$$

Substituting Eq. (6.10) in Eq. (6.38), the quantum kinetic energy can be rewritten as

$$\begin{aligned}\Theta_Q &= -\frac{\hbar^2}{2m^2}\int \sqrt{\rho}\Delta\sqrt{\rho}\, d\mathbf{r} \\ &= \frac{\hbar^2}{2m^2}\int (\nabla\sqrt{\rho})^2\, d\mathbf{r} = \frac{\hbar^2}{8m^2}\int \frac{(\nabla\rho)^2}{\rho}\, d\mathbf{r}.\end{aligned} \tag{6.39}$$

This functional was introduced by von Weizsäcker [79] and is related to the Fisher entropy $S_F = \int (\nabla\rho)^2/\rho\, d\mathbf{r}$ [80]. The third term in Eq. (6.37) is the internal energy

$$U = \frac{2\pi a\hbar^2}{m^3}\int \rho^2\, d\mathbf{r} = \frac{2\pi a\hbar^2}{m}N^2\int |\psi|^4\, d\mathbf{r} \tag{6.40}$$

which is quadratic in ρ and quartic in ψ. The fourth term is the gravitational potential energy of interaction

$$W = \frac{1}{2}\int \rho\Phi \, d\mathbf{r}. \tag{6.41}$$

It is shown in Appendix 6.8 that the total energy is conserved: $\dot{E}_{tot} = 0$. As a result, a minimum of the total energy functional $E_{tot}[\rho, \mathbf{u}]$ at fixed mass determines a steady state of the quantum Euler-Poisson system (6.14)–(6.16) that is formally nonlinearly dynamically stable [81]. Writing the variational principle in the form $\delta E_{tot} - \alpha\delta M = 0$ where α (chemical potential) is a Lagrange multiplier accounting for the mass constraint, and using the results of Appendix 6.8, we obtain $\mathbf{u} = \mathbf{0}$ and the steady state equation (6.20) with $E = m\alpha$. Therefore, the eigenenergy E/m may be interpreted as a chemical potential α.

Remark Since the stable steady states of the quantum Euler-Poisson system are minima of energy E_{tot} at fixed mass, they can be determined by a relaxation method. Indeed, they can be obtained by solving the quantum Smoluchowski-Poisson (SP) system (see Eqs. (120)–(121) of [82]) that decreases the energy E_{tot} at fixed mass (in this context, the quantum SP system is interpreted as a numerical algorithm).

6.2.9 The Virial Theorem

From the quantum Euler-Poisson system (6.14)–(6.16), we can derive the time-dependent Virial theorem (see Appendix 6.9):

$$\frac{1}{2}\ddot{I} = 2(\Theta_c + \Theta_Q) + 3U + W, \tag{6.42}$$

where $I = \int \rho r^2 \, d\mathbf{r}$ is the moment of inertia. At equilibrium ($\ddot{I} = \Theta_c = 0$), we obtain the time-independent Virial theorem

$$2\Theta_Q + 3U + W = 0. \tag{6.43}$$

On the other hand, the total energy reduces to $E_{tot} = \Theta_Q + U + W$. Finally, multiplying the steady state Eq. (6.20) by ρ and integrating over the configuration, we obtain the identity $\Theta_Q + 2U + 2W = NE$. These are exact results valid at equilibrium.

6.3 The Gaussian Ansatz

To obtain the density profile of a self-gravitating BEC and the mass-radius relation, we have to solve the differential Eq. (6.23) expressing the condition of hydrostatic equilibrium. This can be done numerically [16]. However, we can also obtain approximate analytical results by using a Gaussian ansatz [15].

6.3.1 The Total Energy

We shall calculate the energy functional (6.37) by making a Gaussian ansatz

$$\rho(\mathbf{r}) = \frac{M}{R^3}\frac{1}{\pi^{3/2}}e^{-\frac{r^2}{R^2}} \tag{6.44}$$

for the density profile. The central density is $\rho(0) = M/(\pi^{3/2}R^3)$. The radius containing 99 % of the total mass is $R_{99} = 2.38R$. Using Eq. (6.44), the moment of inertia, the quantum kinetic energy, the internal energy, and the gravitational energy are given by

$$I = \alpha MR^2, \quad \Theta_Q = \sigma\frac{\hbar^2 M}{m^2R^2}, \quad U = \zeta\frac{2\pi a\hbar^2M^2}{m^3R^3}, \quad W = -\nu\frac{GM^2}{R} \tag{6.45}$$

with the coefficients $\alpha = 3/2$, $\sigma = 3/4$, $\zeta = 1/(2\pi)^{3/2}$, and $\nu = 1/\sqrt{2\pi}$.

For a density profile of the form $\rho(\mathbf{r}, t) = (M/R(t)^3)f(\mathbf{r}/R(t))$ and for a velocity profile of the form $\mathbf{u}(\mathbf{r}, t) = H(t)\mathbf{r}$, the equation of continuity (6.14) implies that $H = \dot{R}/R$. We then find that the classical kinetic energy is given by $\Theta_c = \frac{1}{2}\alpha M\dot{R}^2$. Regrouping the foregoing expressions, the energy functional (6.37) can be rewritten as a function of R and $\dot{R}$ (for a fixed mass M) as

$$E_{tot} = \frac{1}{2}\alpha M\left(\frac{dR}{dt}\right)^2 + V(R) \tag{6.46}$$

with

$$V(R) = \sigma\frac{\hbar^2M}{m^2R^2} + \zeta\frac{2\pi a\hbar^2M^2}{m^3R^3} - \nu\frac{GM^2}{R}. \tag{6.47}$$

Equation (6.46) may be interpreted as the total energy of a fictive particle with mass αM and position R moving in a potential $V(R)$. The potential $V(R)$ is plotted in Fig. 6.1 in the different cases considered below.

6.3.2 The Mass-Radius Relation

A stable equilibrium state of the quantum Euler-Poisson system (6.14)–(6.16) is a minimum of the energy functional $E_{tot}[\rho, \mathbf{u}]$ given by Eq. (6.37) at fixed mass M. Within the Gaussian ansatz, we are led to determining the minimum of the function $E_{tot}(R, \dot{R})$ given by Eq. (6.46) at fixed mass M. Clearly, we must have $\dot{R} = 0$, implying that a minimum of energy at fixed mass is a steady state. Then, we must determine the minimum of the potential energy $V(R)$. Computing the first derivative of $V(R)$ and setting $V'(R) = 0$, we obtain the mass-radius relation

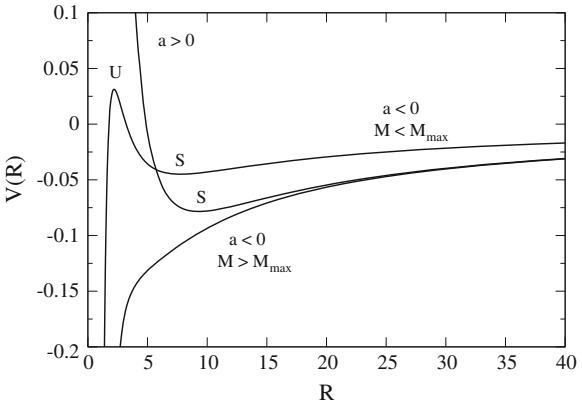

Fig. 6.1 The potential $V(R)$ of the effective mechanical problem

$$M = \frac{2\sigma}{\nu} \frac{\frac{\hbar^2}{Gm^2R}}{1 - \frac{6\pi\zeta a\hbar^2}{\nu Gm^3R^2}}. \tag{6.48}$$

This relation may also be obtained from the equilibrium Virial theorem (6.43) by making the Gaussian ansatz (see Sect. 6.3.3). On the other hand, a critical point of $V(R)$, satisfying $V'(R) = 0$, is an energy minimum if, and only if, $V''(R) > 0$. Computing the second derivative of $V(R)$ and using the mass-radius relation (6.48), we get

$$V''(R) = \frac{\nu GM^2}{R^3}\left(1 + \frac{6\pi\zeta a\hbar^2}{\nu Gm^3R^2}\right). \tag{6.49}$$

Let us consider asymptotic limits of the mass-radius relation:
(i) In the non-interacting case ($a = 0$), we obtain

$$R = \frac{2\sigma}{\nu}\frac{\hbar^2}{GMm^2}. \tag{6.50}$$

This relation results from the balance between the attractive effect of gravity and the repulsive effect of the quantum pressure (Heisenberg's uncertainty principle). This solution is stable because it is an energy minimum ($V''(R) > 0$). The radius R_{99} containing 99 % of the mass is $R_{99} = 8.96\,\hbar^2/GMm^2$. This can be compared with the exact result (6.26) giving $R_{99}^{exact} = 9.95\,\hbar^2/GMm^2$. The agreement is fairly good.
(ii) In the TF approximation when $a > 0$, we get

$$R = \left(\frac{6\pi\zeta}{\nu}\right)^{1/2}\left(\frac{a\hbar^2}{Gm^3}\right)^{1/2}. \tag{6.51}$$

This relation results from the balance between the attractive effect of gravity and the repulsive effect of the scattering (short-range interactions). This solution is stable because it is an energy minimum ($V''(R) > 0$). The radius is independent on the mass. The radius R_{99} containing 99 % of the mass is given by $R_{99} = 4.12(a\hbar^2/Gm^3)^{1/2}$. This can be compared with the exact result (6.31) giving $R_{99}^{exact} = 3.00(a\hbar^2/Gm^3)^{1/2}$. The agreement is less good than in the non-interacting case. The reason is related to the fact that the distribution (6.30) has a compact support so that it is quite different from a Gaussian.

(iii) In the non-gravitational limit when $a < 0$, we get

$$R = \frac{3\pi\zeta}{\sigma}\frac{M|a|}{m}. \tag{6.52}$$

This relation results from the balance between the attractive effect of the scattering and the repulsive effect of the quantum pressure. This solution is unstable because it is an energy maximum ($V''(R) < 0$). The radius R_{99} containing 99 % of the mass is given by $R_{99} = 1.90M|a|/m$.

We now come back to the general case:

(i) We first consider self-gravitating BECs with repulsive short-range interactions ($a > 0$). The mass-radius relation is represented in Fig. 6.2. There exist one, and only one, solution for each value of the mass and it is stable since, according to Eq. (6.49), it is an energy minimum ($V''(R) > 0$); see Fig. 6.1. The radius is a decreasing function of the mass. For $M \to +\infty$, the radius R tends to a minimum value $R_{\rm min}$ given by Eq. (6.51). For $M \to 0$, the radius $R \to +\infty$ with the scaling (6.50). The TF approximation is valid for $M \gg M_a$, i.e. $R \sim R_a \sim R_{\rm min}$ and the non-interacting approximation is valid for $M \ll M_a$, i.e. $R \gg R_a \sim R_{\rm min}$.

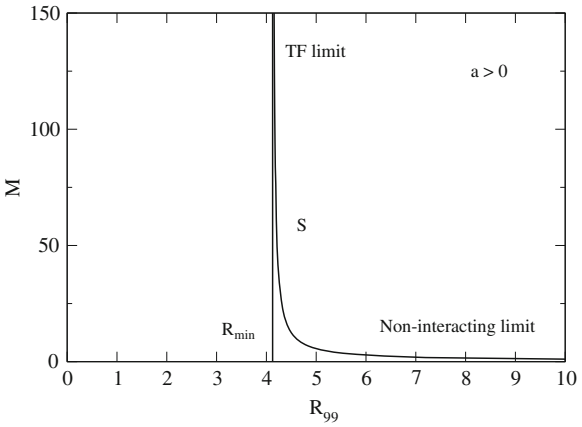

Fig. 6.2 Mass-radius relation of self-gravitating BECs with repulsive self-interaction ($a > 0$). There is a minimum radius $R_{\rm min}$ corresponding to $M \to +\infty$. All the configurations are stable

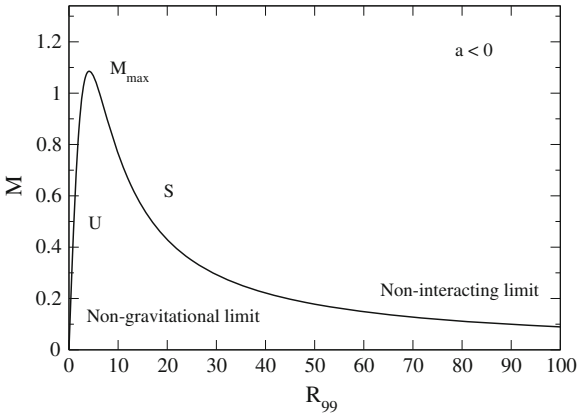

Fig. 6.3 Mass-radius relation of self-gravitating BECs with attractive self-interaction ($a < 0$). There is a maximum mass $M_{\max}$ corresponding to a critical radius R_*. The configurations with $R > R_*$ are stable and the configurations with $R < R_*$ are unstable

(ii) We now consider self-gravitating BECs with attractive short-range interactions ($a < 0$). The mass-radius relation is represented in Fig. 6.3. There exist a maximum mass and a corresponding critical radius

$$M_{\max} = \left(\frac{\sigma^2}{6\pi\zeta\nu}\right)^{1/2} \frac{\hbar}{\sqrt{Gm|a|}}, \quad R_* = \left(\frac{6\pi\zeta}{\nu}\right)^{1/2} \left(\frac{|a|\hbar^2}{Gm^3}\right)^{1/2}. \tag{6.53}$$

They are related to each other by $M_{\max} = (\sigma/\nu)\hbar^2/Gm^2R_*$. The approximate values $M_{\max} = 1.08\hbar/\sqrt{Gm|a|}$ and $R_{99}^* = 4.13(|a|\hbar^2/Gm^3)^{1/2}$ obtained with the Gaussian ansatz [15] are in fairly good agreement with the exact results $M_{\max}^{exact} = 1.01\hbar/\sqrt{Gm|a|}$ and $(R_{99}^*)^{exact} = 5.5(|a|\hbar^2/Gm^3)^{1/2}$ obtained numerically [16]. For $M > M_{\max}$, there is no equilibrium state (no critical point of energy) and the system undergoes gravitational collapse (see Fig. 6.4). Since quantum mechanics (Heisenberg's uncertainty principle) cannot arrest gravitational collapse, the self-gravitating BEC is expected to form a black hole. For $M < M_{\max}$, there exist two solutions with the same mass. However, according to Eq. (6.49), only the solution with the largest radius $R > R_*$ is stable (minimum of energy $V''(R) > 0$). The other solution is an unstable maximum of energy ($V''(R) < 0$); see Fig. 6.1. We can check that the change of stability ($V''(R) = 0$) occurs at the turning point of mass ($M'(R) = 0$) in agreement with the Poincaré theory of linear series of equilibria and with the theory of catastrophes (see [15] for more details). On the stable branch, the radius is a decreasing function of the mass. The non-interacting approximation is valid for $M \ll M_a \sim M_{\max}$ with $R \gg R_a \sim R_*$. For $M \to 0$, the radius $R \to +\infty$ with the scaling (6.50). For $M \to M_{\max}$, the radius R tends to the minimum stable value R_*. On the unstable branch, the radius is an increasing function of the mass. The non-gravitational approximation is valid for $M \ll M_a \sim M_{\max}$ with $R \ll R_a \sim R_*$.

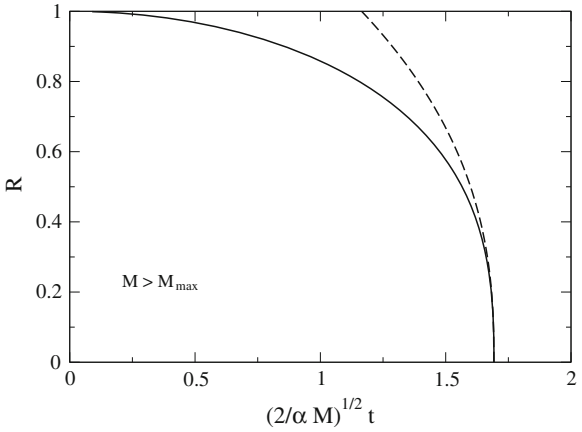

Fig. 6.4 Collapse of a self-gravitating BEC with attractive self-interaction ($a < 0$) when $M > M_{\rm max}$. We have represented the BEC radius $R(t)$ as a function of time by solving Eq. (6.54) starting from a configuration with a radius R_0 and without velocity ($\dot{R}_0 = 0$). The solution is $(2/\alpha M)^{1/2} t = \int_{R(t)}^{R_0} dR/\sqrt{V(R_0) - V(R)}$ (*solid line*). The collapse generates a finite time singularity, i.e. the radius vanishes in a finite time. The collapse time t_{coll} is obtained from the foregoing expression by setting $R(t_{coll}) = 0$ giving $(2/\alpha M)^{1/2} t_{coll} = \int_0^{R_0} dR/\sqrt{V(R_0) - V(R)}$. The solution can then be rewritten as $(2/\alpha M)^{1/2}(t_{coll} - t) = \int_0^{R(t)} dR/\sqrt{V(R_0) - V(R)}$. In the figure, we have taken $M = 1.2, R_0 = 1$, and $M_{\rm max} = 1.08$ yielding $(2/\alpha M)^{1/2} t_{coll} = 1.69$. For $t \to t_{coll}$, the collapse is only driven by the attractive self-interaction and the radius behaves as $R(t) \simeq (25\pi\zeta|a|\hbar^2 M/\alpha m^3)^{1/5}(t_{coll} - t)^{2/5}$ (*dashed line*). This scaling is different from the scaling $R(t) \propto (t_{coll} - t)^{1/2}$ obtained by directly solving the non-gravitational GP equation with an attractive self-interaction [83]. Therefore, the Gaussian ansatz is not qualitatively accurate to describe the collapse of a BEC

For $M \to 0$, the radius $R \to 0$ with the scaling (6.52). However, these configurations are inaccessible since they are dynamically unstable (energy maxima). If the system is initially placed on the unstable branch ($R_U < R_*$), it can either (i) undergo gravitational collapse ($R(t) \to 0$), (ii) evaporate ($R(t) \to +\infty$) if its energy E_{tot} is positive[2] or (iii) oscillate around the stable equilibrium state with a larger radius ($R_S > R_*$) if its energy E_{tot} is negative; see Fig. 6.1. It may also relax towards the stable equilibrium state with a larger radius ($R(t) \to R_S > R_*$) provided that it is able to dissipate energy, e.g. by radiation or due to some damping. On the other hand, since the stable states are only *metastable* (local minima of energy), due to classical or quantum fluctuations (tunneling effect), the system initially put in a metastable state may cross the barrier of potential played by the unstable state and ultimately collapse.

[2] Using Eq. (51) of [16] obtained with the Gaussian ansatz, we find that $E_{tot} > 0$ when $M < (\sqrt{3}/2)M_{\rm max}$ and $R < R_*/\sqrt{3}$.

6.3.3 The Virial Theorem

Using the Gaussian ansatz, the time-dependent Virial theorem (6.42) can be written after simplification as [15]:

$$\alpha M \frac{d^2R}{dt^2} = -\frac{dV}{dR}. \tag{6.54}$$

This equation describes the motion of a fictive particle with mass αM and position R in a potential $V(R)$. From Eq. (6.54), we find that the total energy $E_{tot} = \Theta_c + V$ defined by Eq. (6.46) is conserved: $\dot{E}_{tot} = 0$. The equilibrium Virial theorem ($d^2R/dt^2 = 0$) returns the mass-radius relation (6.48) obtained from the condition $dV/dR = 0$. In this mechanical analogy, a stable equilibrium state corresponds to a *minimum* of $V(R)$ as we have previously indicated.

6.3.4 The Pulsation Equation

To study the linear dynamical stability of a steady state of Eq. (6.54), we make a small perturbation about that state and write $R(t) = R + \varepsilon(t)$ where R is the equilibrium radius and $\varepsilon(t) \ll R$ is the perturbation. Using $V'(R) = 0$ and keeping only terms that are linear in ε, we obtain the equation

$$\frac{d^2\varepsilon}{dt^2} + \omega^2 \varepsilon = 0, \tag{6.55}$$

where ω is a complex pulsation given by

$$\omega^2 = \frac{1}{\alpha M} V''(R). \tag{6.56}$$

A steady state is linearly stable if, and only if, $\omega^2 > 0$; that is to say if, and only if, it is a (local) minimum of energy $V(R)$. In that case, the system oscillates about its equilibrium with a pulsation ω. Otherwise, the perturbation grows exponentially rapidly with a growth rate $\lambda_+ = \sqrt{-\omega^2} > 0$ (the other mode is damped at a rate $\lambda_- = -\sqrt{-\omega^2} < 0$). Computing $V''(R)$ from Eq. (6.47), and using Eq. (6.45), we find that

$$\omega^2 = \frac{6\Theta_Q + 12U + 2W}{I}. \tag{6.57}$$

In the non-interacting case ($U = 0$), using the Virial theorem (6.43), we get $\omega^2 = -W/I$. In the TF approximation ($\Theta_Q = 0$), using the Virial theorem (6.43), we obtain $\omega^2 = -2W/I$. This expression coincides with the Ledoux formula $\omega^2_{Ledoux} = (4 - 3\gamma)W/I$ [84] for a polytrope of index $\gamma = 2$. Using the Gaussian ansatz, we obtain $\omega = (\nu/\alpha)^{1/2} t_D^{-1} = 0.516\, t_D^{-1}$ in the non-interacting case and $\omega =$

$(2\nu/\alpha)^{1/2}t_D^{-1} = 0.729\, t_D^{-1}$ in the TF approximation, where $t_D = (R^3/GM)^{1/2}$ is the dynamical time.

From Eqs. (6.48), (6.49) and (6.56), we obtain the nice identity

$$\frac{dM}{dR} = -\frac{1}{2\sigma}\frac{m^2R^3}{\hbar^2}V''(R) = -\frac{\alpha}{2\sigma}\frac{m^2MR^3}{\hbar^2}\omega^2. \tag{6.58}$$

This identity relates the slope of the mass-radius relation $M(R)$ to the complex pulsation ω. It first shows that a change of stability ($\omega = 0$) occurs at a turning point of mass ($dM/dR = 0$). Furthermore, it shows that a branch with a negative slope ($dM/dR < 0$) is stable ($\omega^2 > 0$) whereas a branch with a positive slope ($dM/dR > 0$) is unstable. This is an illustration of the Poincaré turning point criterion.

6.4 Application of Newtonian Self-gravitating BECs to Dark Matter Halos

In this section, we apply the model of Newtonian self-gravitating BECs to dark matter halos. In the numerical applications, we consider a typical dark matter halo of mass $M = 3\times 10^{11}M_\odot$, radius $R = 10\,\mathrm{kpc} = 3.09\times 10^{20}\,\mathrm{m}$, density $\rho = M/R^3 = 2.02\times 10^{-23}\,\mathrm{g/cm^3}$, and dynamical time $t_D = 1/\sqrt{G\rho} = 27\,\mathrm{Myrs}$.

6.4.1 The Non-interacting Case

In the non-interacting case ($a = 0$), the typical radius of a self-gravitating BEC is given by Eq. (6.32). It may be rewritten as

$$\frac{R_Q}{1\,\mathrm{kpc}} = 8.54\times 10^{-37}\,\frac{M_\odot}{M}\left(\frac{1\,\mathrm{eV}/c^2}{m}\right)^2. \tag{6.59}$$

The exact radius of a self-gravitating BEC without self-interaction containing 99 % of the mass is $R_{99} = 9.95R_Q$. In order to reproduce the typical scales of dark matter halos, the mass of the bosons must be of the order of $m = 1.68\times 10^{-24}\,\mathrm{eV}/c^2$ [17]. Such an ultralight particle corresponds to "fuzzy cold dark matter" [23].

6.4.2 The Thomas-Fermi Approximation

In the TF approximation, the typical radius of a self-gravitating BEC with a repulsive self-interaction ($a > 0$) is given by Eq. (6.33). It may be rewritten as

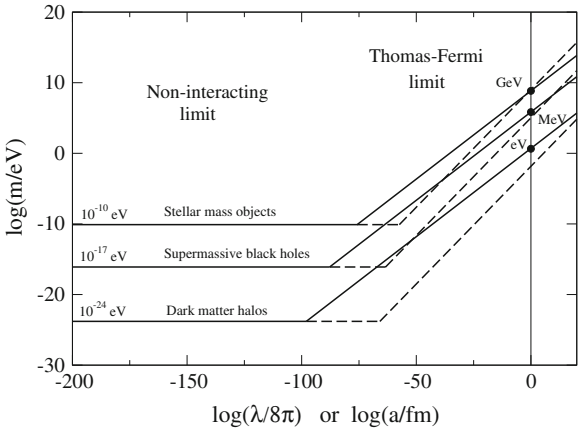

Fig. 6.5 Relation between the boson mass m and the self-interaction constant λ (*solid lines*) or the scattering length a (*dashed lines*) in order to reproduce the typical scales of dark matter halos, supermassive black holes, and stellar mass objects (neutron stars, Machos. . .). One can see that the TF approximation is valid even for very small values of a and λ, and that the self-interaction can considerably increase the required value of the boson mass as discussed in the text

$$\frac{R_a}{1\,\mathrm{kpc}} = 5.56\times 10^{-3}\left(\frac{a}{1\,\mathrm{fm}}\right)^{1/2}\left(\frac{1\,\mathrm{eV}/c^2}{m}\right)^{3/2}, \tag{6.60}$$

$$\frac{R_a}{1\,\mathrm{kpc}} = 78.1\sqrt{\frac{\lambda}{8\pi}}\left(\frac{1\,\mathrm{eV}/c^2}{m}\right)^{2}. \tag{6.61}$$

The exact radius of a self-gravitating BEC with a repulsive self-interaction in the TF approximation is $R = \pi R_a$. In order to reproduce the typical scales of dark matter halos, the mass of the bosons must be of the order of

$$\frac{m}{1\,\mathrm{eV}/c^2} = 1.45\times 10^{-2}\left(\frac{a}{1\,\mathrm{fm}}\right)^{1/3}, \quad \frac{m}{1\,\mathrm{eV}/c^2} = 4.95\left(\frac{\lambda}{8\pi}\right)^{1/4}. \tag{6.62}$$

For $a = 10^6\,\mathrm{fm}$, which corresponds to the typical value of the scattering length observed in laboratory BEC experiments [49], this gives a mass $m = 1.45\,\mathrm{eV/c^2}$ [40] much larger than in the non-interacting case (see Sect. 6.4.1). The corresponding value of the self-interaction constant is $\lambda/8\pi = 7.35\times 10^{-3}$. Therefore, a self-interaction $\lambda \sim 1$ can increase the required value of the boson mass from $m \sim 10^{-24}\,\mathrm{eV}/c^2$ to $m \sim 1\,\mathrm{eV}/c^2$ (see Fig. 6.5) which may be more realistic from a particle physics point of view.

It is important to realize that the radius R of a self-interacting BEC directly determines the ratio a/m^3 or λ/m^4. For a typical dark matter halo, we obtain $m^3/a = 3.05\times 10^{-6}\,(\mathrm{eV/c^2})^3/\mathrm{fm}$ and $m^4/\lambda = 23.9\,(\mathrm{eV}/c^2)^4$. Inversely, the specification of m and a (or λ) determines the radius of the halo.

6.4.3 Validity of the Thomas-Fermi Approximation

The TF approximation is valid when $M \gg M_a$ where M_a is the characteristic mass given by Eq. (6.35). It may be rewritten as

$$\frac{M_a}{M_\odot} = 1.54\times 10^{-34}\left(\frac{1\,\mathrm{fm}}{|a|}\right)^{1/2}\left(\frac{1\,\mathrm{eV}/c^2}{m}\right)^{1/2}, \quad \frac{M_a}{M_\odot} = 1.09\times 10^{-38}\sqrt{\frac{8\pi}{|\lambda|}}. \tag{6.63}$$

For a typical dark matter halo, the TF approximation is valid when [15, 16]:

$$\frac{m}{1\,\mathrm{eV}/c^2} \gg 2.63\times 10^{-91}\frac{1\,\mathrm{fm}}{|a|}, \quad \frac{|\lambda|}{8\pi} \gg 1.33\times 10^{-99}. \tag{6.64}$$

Therefore, the TF approximation is valid even for an extremely (!) small value of a or λ fulfilling the condition (6.64). According to Eq. (6.36), this is due to the smallness of $(M_P/M)^2$. For the values $a = 10^6$ fm, $m = 1.45\,\mathrm{eV/c^2}$, and $\lambda/8\pi = 7.35\times 10^{-3}$ considered in [40], the condition (6.64) is fulfilled by more than 90 orders of magnitude so that the TF approximation is perfect. In that case, the density profile (6.30) is steady and stable. Alternatively, for the values $m \sim 10^{-24}\,\mathrm{eV}/c^2$, $a \sim 10^{-67}$ fm, and $\lambda/8\pi \sim 10^{-99}$ considered in [44], the TF approximation is not valid. This is the reason why the authors of [48] find that the profile (6.30) is not steady in that case. Indeed, the TF condition on which this profile is based is not satisfied. Note that the general dark matter halo profile that is the solution of the full condition of hydrostatic equilibrium (6.21) has been calculated numerically in [16] for different values of a and m. This calculation does not make any approximation.

6.4.4 The Case of Attractive Self-interactions

For a self-gravitating BEC with an attractive self-interaction ($a < 0$), there exist a maximum mass $M_{\max} = 1.01M_a$. The corresponding radius containing 99 % of the mass is $R^*_{99} = 5.5R_a$. This can be rewritten as [15, 16]:

$$M_{\max} = 1.01\frac{M_P}{\sqrt{\frac{|\lambda|}{8\pi}}}, \quad R^*_{99} = 5.5\sqrt{\frac{|\lambda|}{8\pi}}\frac{M_P}{m}\lambda_c. \tag{6.65}$$

If $|\lambda| \sim 1$ the maximum mass is of the order of the Planck mass $M_P = 2.18\times 10^{-8}$ kg. Of course, this is ridiculously small at the scale of dark matter halos meaning that a self-gravitating BEC with an attractive self-interaction is extremely unstable. The maximum mass (6.65) becomes of the order of the typical mass of dark matter halos

for $|\lambda|/8\pi = 1.36 \times 10^{-99}$. The corresponding radius is of the order of the typical radius of dark matter halos provided that $m = 1.26 \times 10^{-24}\,\mathrm{eV/c^2}$. This corresponds to a scattering length $|a| = 2.13 \times 10^{-67}\,\mathrm{fm}$.

Let us consider a self-gravitating BEC without self-interaction ($\lambda = 0$) representing a typical dark matter halo of mass $M = 3 \times 10^{11} M_\odot$. This halo is stable. We now assume that the bosons have a small attractive self-interaction ($\lambda < 0$). The halo becomes unstable when $M > M_{\rm max}$. Using Eq. (6.65), we find that the dark matter halo becomes unstable as soon as

$$\frac{|a|}{1\,\mathrm{fm}} > 2.69 \times 10^{-91} \frac{1\,\mathrm{eV}/c^2}{m}, \quad \frac{|\lambda|}{8\pi} > 1.36 \times 10^{-99}. \tag{6.66}$$

Therefore, a very small attractive self-interaction can destabilize a dark matter halo. This shows that no self-interaction ($\lambda = 0$) is very different from a small self-interaction ($\lambda \to 0$). For $m = 1.68 \times 10^{-24}\,\mathrm{eV}/c^2$, we find that the halo becomes unstable when $|a| > 1.60 \times 10^{-67}\,\mathrm{fm}$. In that case, it forms a black hole.

In we assume $|\lambda| \sim 1$, we find that $M_{\rm max} \sim M_P$ and, consequently, $M \gg M_{\rm max}$ for dark matter halos. Therefore, we can make the TF approximation and neglect the effect of the quantum pressure. In that case, the BEC collapses due to the effect of self-gravity and attractive scattering (see Fig. 6.4). Since quantum mechanics (Heisenberg's uncertainty principle) cannot stabilize the BEC against gravitational collapse, this process can lead to a supermassive black hole (of course, close to the singularity, the Newtonian approximation is not relevant anymore and we must use general relativity). For the numerical application, we take $a = -10^6\,\mathrm{fm}$ which corresponds to the typical scattering length of ^{7}Li atoms in laboratory BEC experiments [49]. We also take a boson mass $m = 1.45\,\mathrm{eV/c^2}$ as in Sect. 6.4.2. This gives a self-interaction constant $\lambda/8\pi = -7.35 \times 10^{-3}$. The maximum mass is $M_{\rm max} = 1.29 \times 10^{-37} M_\odot$ much smaller than the mass $M = 3 \times 10^{11} M_\odot$ of dark matter halos. If we consider a configuration with an initial radius $R_0 = 10\,\mathrm{kpc}$, we find that the collapse time is of the order of $t_D \sim 1/(GM/R_0^3)^{1/2} \sim 27\,\mathrm{Myrs}$. To be specific, we have taken the parameters of Sect. 6.4.2 by just reverting the sign of a. Other numerical applications with a total mass $M \sim 10^6 M_\odot$ of the order of the mass of supermassive black holes, and a smaller initial radius R_0, could be more relevant.

6.5 Application of General Relativistic BECs to Neutron Stars, Dark Matter Stars, and Black Holes

The Newtonian approximation is valid when the radius R of a configuration with mass M is much larger than the Schwarzschild radius $R_S = 2GM/c^2$ or, equivalently, when $M \ll Rc^2/G$. This condition can be rewritten as $M/M_\odot \ll 0.677R/\mathrm{km}$. For a typical dark matter halo, the term in the left hand side is of order 10^{11} while the term in the right hand side is of order 10^{17}. Therefore, this condition is fulfilled by 6 orders of magnitude so that the Newtonian approximation is very good for dark matter halos.

By contrast, for compact objects similar to neutron stars for which $M \sim 1M_\odot$ and $R \sim 10\,\mathrm{km}$ (yielding a typical density $\rho \sim M/R^3 \sim 2\times 10^{15}\,\mathrm{g/cm^3}$ and a dynamical time $t_D \sim 1/\sqrt{G\rho} \sim 10^{-4}\,\mathrm{s}$), we must use general relativity.

6.5.1 Non-interacting Boson Stars

In the absence of short-range interaction, the mass-radius relation of a non-relativistic self-gravitating BEC is given by Eq. (6.26). This relation is valid as long as the radius is much larger than the Schwarzschild radius $R_S = 2GM/c^2$. Equating the two relationships, and introducing the Planck mass, we obtain the scaling of the maximum mass of a relativistic self-gravitating BEC without self-interaction

$$M_Q^r = \frac{\hbar c}{Gm} = \frac{M_P^2}{m}. \tag{6.67}$$

The exact value of the maximum mass of non-interacting boson stars was determined by Kaup [51] by solving the Klein-Gordon-Einstein equations. It is given by $M_{\rm max}^Q = 0.633M_Q^r$. The radius $R_Q^r = GM_Q^r/c^2$ corresponding to Eq. (6.67) is

$$R_Q^r = \frac{\hbar}{mc} = \lambda_c. \tag{6.68}$$

It scales as the Compton wavelength of the particles that compose the BEC. More precisely, the exact minimum radius of non-interacting boson stars containing 95 % of the mass is given by $R_{\rm min}^Q = 6.03R_Q^r$ [60]. The maximum mass and the minimum radius are related to each other by $R_{\rm min}^Q = 9.53GM_{\rm max}^Q/c^2$. The Newtonian approximation is valid when $M \ll M_{\rm max}^Q$ and $R \gg R_{\rm min}^Q$.

The typical mass and typical radius of non-interacting boson stars may be rewritten as

$$\frac{M_Q^r}{M_\odot} = 1.34\times 10^{-10}\,\frac{\mathrm{eV}/c^2}{m}, \quad \frac{R_Q^r}{\mathrm{km}} = 1.48\frac{M_Q^r}{M_\odot}. \tag{6.69}$$

For $m \sim 1\,\mathrm{GeV}/c^2$, corresponding to the typical mass of the neutrons, the Kaup mass $M_{\rm max}^Q \sim 10^{-19}M_\odot \sim 10^{11}\,\mathrm{kg}$ and the Kaup radius $R_{\rm min}^Q \sim 10^{-19}\,\mathrm{km}$ are very small. This describes mini boson stars. They have the characteristics of primordial black holes whose lifetime is of the order of the present age of the universe (∼3 billion years) [85]. These mini boson stars could play a role for dark matter if they exist in the universe in abundance.

The Kaup mass becomes of the order of the solar mass if the bosons have a mass $m \sim 10^{-10}\,\mathrm{eV}/c^2$ (leading to a Kaup radius of the order of the km). For example, axionic boson stars could account for the mass of MACHOs (between 0.3 and $0.8M_\odot$) if the axions have such a small mass [68].

For dark matter halos modeled as non-interacting BECs with a boson mass $m \sim 10^{-24}\,\mathrm{eV}/c^2$ (see Sect. 6.4.1), we find that $M^Q_{\max} \sim 10^{14} M_\odot$ much larger than the typical mass of dark matter halos $M \sim 10^{11} M_\odot$. Therefore, the Newtonian approximation can be used for dark matter halos since $M \ll M^Q_{\max}$.

6.5.2 The Thomas-Fermi Approximation for Boson Stars

In the TF approximation, the radius of a non-relativistic self-gravitating BEC with repulsive self-interaction ($a > 0$) is given by Eq. (6.31). It is independent on the mass M. The Newtonian approximation is valid as long as the radius (6.31) is much larger than the Schwarzschild radius $R_S = 2GM/c^2$. Equating these two relationships, and introducing the Planck mass, we obtain the scaling of the maximum mass of a relativistic self-gravitating BEC with repulsive self-interaction in the TF approximation

$$M^r_a = \frac{\hbar c^2 \sqrt{a}}{(Gm)^{3/2}} = \sqrt{\frac{\lambda}{8\pi}} \frac{1}{m^2} \left(\frac{\hbar c}{G}\right)^{3/2} = \sqrt{\frac{\lambda}{8\pi}} \frac{M_P^3}{m^2}. \tag{6.70}$$

The exact value of the maximum mass of a boson star in the TF approximation was determined by Colpi et al. [56] by solving the Klein-Gordon-Einstein equations and by Chavanis and Harko [73] by solving the Tolman-Oppenheimer-Volkoff (TOV) equation with an appropriate equation of state. It is given by $M^a_{\max} = 0.500 M^r_a$ if we use a non-relativistic equation of state and by $M^a_{\max} = 0.307 M^r_a$ if we use a relativistic equation of state [73]. For $\lambda \sim 1$, the maximum mass of self-interacting boson stars scales as the Oppenheimer-Volkoff maximum mass M_P^3/m^2 of neutron stars while the Kaup maximum mass of non-interacting boson stars scales as M_P^2/m. Therefore, in the presence of self-interaction, the maximum mass of a boson star is much larger than the Kaup mass by a factor $M_P/m \gg 1$, so that it becomes astrophysically relevant.

The radius $R^r_a = GM^r_a/c^2$ corresponding to Eq. (6.70) is given by

$$R^r_a = \left(\frac{a\hbar^2}{Gm^3}\right)^{1/2} = \left(\frac{\lambda \hbar^3}{8\pi G m^4 c}\right)^{1/2} = \sqrt{\frac{\lambda}{8\pi}} \frac{M_P}{m} \lambda_c \tag{6.71}$$

as in the Newtonian approximation. The exact minimum radius of a relativistic self-gravitating BEC with repulsive self-interactions in the TF approximation is given by $R^a_{\min} = 1.89 R^r_a$ for a non-relativistic equation of state and by $R^a_{\min} = 1.92 R^r_a$ for a relativistic equation of state [73]. For $\lambda \sim 1$, the radius of a self-interacting BEC is much larger than the Compton wavelength since $M_P/m \gg 1$. The maximum mass and the minimum radius are related to each other by $R^a_{\min} = 3.78 G M^a_{\max}/c^2$ for a non-relativistic equation of state and by $R^a_{\min} = 6.25\, G M^a_{\max}/c^2$ for a relativistic equation of state. The Newtonian approximation is valid when $M \ll M^a_{\max}$ and $R \gg R^a_{\min}$.

The previous equations may be rewritten as

$$\frac{M_a^r}{M_\odot} = 3.66 \left(\frac{a}{\mathrm{fm}}\right)^{1/2} \left(\frac{\mathrm{GeV}/c^2}{m}\right)^{3/2}, \tag{6.72}$$

$$\frac{M_a^r}{M_\odot} = 1.62 \sqrt{\frac{\lambda}{8\pi}} \left(\frac{\mathrm{GeV}/c^2}{m}\right)^{2}, \quad \frac{R_a^r}{\mathrm{km}} = 1.48 \frac{M_a^r}{M_\odot}. \tag{6.73}$$

For $m \sim 1\,\mathrm{GeV}/c^2$, corresponding to the typical mass of the neutrons, and $a \sim 1$ fm corresponding to $\lambda \sim 1$, the maximum mass M_{max}^a of self-interacting boson stars is of the order of the solar mass, and their corresponding radius R_{min}^a is of the order of the kilometer, as in the case of neutron stars. These parameters could describe boson stars with relevant masses.

We emphasize that the mass M or the radius R of a self-interacting boson star directly determines the ratio a/m^3 or λ/m^4. Taking $M = 1\,M_\odot$, we obtain $m^3/a = 3.35\,(\mathrm{GeV/c^2})^3/\mathrm{fm}$ and $m^4/\lambda = 2.61 \times 10^{-2}\,(\mathrm{GeV}/c^2)^4$ for a non-relativistic equation of state and $m^3/a = 1.26\,(\mathrm{GeV/c^2})^3/\mathrm{fm}$ and $m^4/\lambda = 9.84 \times 10^{-3}\,(\mathrm{GeV}/c^2)^4$ for a relativistic equation of state.

In order to reproduce the typical mass $M \sim 1\,M_\odot$ of neutron stars, the mass of the bosons must be of the order of

$$\frac{m}{1\,\mathrm{GeV}/c^2} = 1.50 \left(\frac{a}{1\,\mathrm{fm}}\right)^{1/3}, \quad \frac{m}{1\,\mathrm{GeV}/c^2} = 0.900 \left(\frac{\lambda}{8\pi}\right)^{1/4} \tag{6.74}$$

for a non-relativistic equation of state and

$$\frac{m}{1\,\mathrm{GeV}/c^2} = 1.08 \left(\frac{a}{1\,\mathrm{fm}}\right)^{1/3}, \quad \frac{m}{1\,\mathrm{GeV}/c^2} = 0.705 \left(\frac{\lambda}{8\pi}\right)^{1/4} \tag{6.75}$$

for a relativistic equation of state. For $a \sim 1$ fm, this gives a mass $m \sim 1\,\mathrm{GeV/c^2}$ much larger than in the non-interacting case (see Sect. 6.5.1). This corresponds to a self-interaction constant $\lambda \sim 1$. Therefore, a self-interaction $\lambda \sim 1$ can increase the required value of the boson mass from $m \sim 10^{-10}\,\mathrm{eV}/c^2$ to $m \sim 1\,\mathrm{GeV}/c^2$ (see Fig. 6.5).

For dark matter halos modeled as self-interacting BECs in the TF approximation with a boson mass $m \sim 1\,\mathrm{eV/c^2}$ and a scattering length $a \sim 10^6$ fm (see Sect. 6.4.2) we find that $M_{\mathrm{max}}^a \sim 10^{17} M_\odot$ much larger than the typical mass of dark matter halos $M \sim 10^{11} M_\odot$. Therefore, the Newtonian approximation can be used for dark matter halos since $M \ll M_{\mathrm{max}}^a$.

6.5.3 Validity of the Thomas-Fermi Approximation

The TF approximation is valid when $M_a^r \gg M_Q^r$ or $R_a^r \gg R_Q^r$. It is convenient to introduce the dimensionless parameter

$$\Lambda = \frac{|a|c^2}{Gm} = \frac{|\lambda|}{8\pi}\frac{\hbar c}{Gm^2} = \frac{|\lambda|}{8\pi}\frac{M_P^2}{m^2}. \tag{6.76}$$

The TF approximation is valid when $\Lambda \gg 1$ and the non-interacting approximation is valid when $\Lambda \ll 1$. For a given value of m, the TF approximation is valid when

$$|a| \gg \frac{Gm}{c^2}, \quad \frac{|\lambda|}{8\pi} \gg \frac{Gm^2}{c\hbar} = \frac{m^2}{M_P^2}. \tag{6.77}$$

For a given value of a or λ, the TF approximation is valid when

$$m \ll \frac{|a|c^2}{G}, \quad m \ll \left(\frac{|\lambda|c\hbar}{8\pi G}\right)^{1/2} = \sqrt{\frac{|\lambda|}{8\pi}}M_P. \tag{6.78}$$

These conditions may be rewritten as

$$\frac{|a|}{1\,\text{fm}}\frac{1\,\text{GeV}/c^2}{m} \gg 1.32\times 10^{-39}, \quad \frac{|\lambda|}{8\pi}\left(\frac{1\,\text{GeV}/c^2}{m}\right)^2 \gg 6.71\times 10^{-39}. \tag{6.79}$$

Therefore, the TF approximation is valid even for an extremely (!) small value of λ fulfilling the condition (6.79). According to Eq. (6.77), this is due to the smallness of m^2/M_P^2. For the values of a, m, and λ given in the previous section, the condition (6.79) is fulfilled by more than 30 orders of magnitude, so that the TF approximation is perfect.

6.5.4 An Interpolation Formula Between the Non-interacting Case and the TF Approximation

The mass-radius relation of a non-relativistic self-gravitating BEC with repulsive short-range interactions may be approximated by

$$M = 9.95\frac{\frac{\hbar^2}{Gm^2R}}{1-8.99\frac{a\hbar^2}{Gm^3R^2}}. \tag{6.80}$$

To obtain this expression, we have used Eq. (6.48) based on the Gaussian ansatz and we have adapted the numerical factors in order to recover the exact results in the

non-interacting case and in the TF limit (the radius R represents the radius containing 99 % of the mass). In the relativistic regime, equating the radius R with the Schwarzschild radius $R_S = 2GM/c^2$, we obtain the following approximate expressions for the maximum mass and the minimum radius of a relativistic self-gravitating BEC with repulsive short-range interactions

$$M_{\rm max} = 0.633\sqrt{1+c_1\Lambda}\frac{M_P^2}{m}, \quad R_{\rm min} = 6.03\sqrt{1+c_2\Lambda}\lambda_c, \tag{6.81}$$

where $(c_1, c_2) = (0.624, 0.0982)$ for a non-relativistic equation of state and $(c_1, c_2) = (0.235, 0.101)$ for a relativistic equation of state. Again, the numerical factors have been adapted in order to recover the exact results in the non-interacting case and in the TF limit (the radius R represents the radius containing 95 % of the mass).

When $M > M_{\rm max}$, there is no equilibrium state and the self-gravitating BEC is expected to collapse and form a black hole. When $M < M_{\rm max}$, there exist stable equilibrium states with $R > R_{\rm min}$ that correspond to boson stars for which gravitational collapse is prevented by quantum mechanics.

6.5.5 Application to Supermassive Black Holes

It has been proposed by certain authors [67, 69, 72] that stable boson stars could mimic supermassive black holes that reside at the center of galaxies. In the absence of self-interaction, the mass of the bosons must be of the order of $m = 3.25 \times 10^{-17}\,{\rm eV}/c^2$ in order to reproduce the mass $M = 2.61 \times 10^6 M_\odot$ of Sgr A* [69]. The corresponding boson star radius is $R = 3.68 \times 10^7$ km. These ultralight bosons could appear in very recent phase transitions and belong to the Goldstone sector. For self-interacting bosons with $\lambda \sim 1$ the required mass is raised from $m \sim 10^{-17}$ to $m \sim 1\,{\rm MeV/c^2}$ [67] (see Fig. 6.5). More generally, in order to reproduce the typical mass $M \sim 10^6 M_\odot$ of supermassive black holes, the mass of the bosons must be of the order of

$$\frac{m}{1\,{\rm MeV}/c^2} = 0.150\left(\frac{a}{1\,{\rm fm}}\right)^{1/3}, \quad \frac{m}{1\,{\rm MeV}/c^2} = 0.9\left(\frac{\lambda}{8\pi}\right)^{1/4} \tag{6.82}$$

for a non relativistic equation of state and

$$\frac{m}{1\,{\rm MeV}/c^2} = 0.108\left(\frac{a}{1\,{\rm fm}}\right)^{1/3}, \quad \frac{m}{1\,{\rm MeV}/c^2} = 0.705\left(\frac{\lambda}{8\pi}\right)^{1/4} \tag{6.83}$$

for a relativistic equation of state. These intermediate mass bosons could appear during cosmological evolution (e.g., soft inflationary events). Finally, if the boson mass is comparable to the Higgs mass ($\sim$125 GeV$/c^2$), then the center of the galaxy

could be a non-topological soliton star [86]. The Higgs particle could be a natural candidate as constituent of a boson condensation if the phase transition occurred in early epochs.

Furthermore, it has been shown that boson stars with $m = 1.2 \times 10^{-16}\,\mathrm{eV}/c^2$, $M = 2.8 \times 10^6 M_\odot$ and $\Lambda = 20$ can mimic the spectrum of an accretion disk produced by a Schwarzschild black hole with the same mass [72] (while boson stars with $\Lambda = 0$ show a hardening of the spectrum at high frequencies [87]). Therefore, it was suggested that boson stars with a small self-interaction can be black hole candidates [72].

6.5.6 Application to Neutron Stars and Dark Matter Stars

According to the study of Chavanis and Harko [73], the maximum mass and minimum radius of general relativistic BEC stars in the TF limit are

$$\frac{M^a_{\rm max}}{M_\odot} = 1.83\left(\frac{a}{\rm fm}\right)^{1/2}\left(\frac{\mathrm{GeV}/c^2}{m}\right)^{3/2}, \quad \frac{R^a_{\rm min}}{\rm km} = 5.59\,\frac{M^a_{\rm max}}{M_\odot} \tag{6.84}$$

for a non-relativistic equation of state and

$$\frac{M^a_{\rm max}}{M_\odot} = 1.12\left(\frac{a}{\rm fm}\right)^{1/2}\left(\frac{\mathrm{GeV}/c^2}{m}\right)^{3/2}, \quad \frac{R^a_{\rm min}}{\rm km} = 9.26\,\frac{M^a_{\rm max}}{M_\odot} \tag{6.85}$$

for a relativistic equation of state. The mass-radius relation is represented in Fig. 6.6. It is parameterized by the central density of the star. For a relativistic equation of state, it has a snail-like structure as in the case of neutron stars modeled by the ideal Fermi gas [74, 88, 89]. This is because the equation of state becomes linear ($p = \rho c^2/3$) in the ultra-relativistic regime (high central densities) [90]. In the non-relativistic regime (low central densities) we recover the Newtonian radius (6.31) that corresponds here to a maximum radius. Using the Poincaré theory, or the theory of catastrophes, one can show that the series of equilibria becomes unstable after the turning point of mass ($M'(R) = 0$) so that only configurations with $M < M^a_{\rm max}$ and $R^a_{\rm min} < R < R_{\rm max}$ are stable.

Chavanis and Harko [73] have proposed that, due to the superfluid properties of the core of neutron stars, the neutrons (fermions) could form Cooper pairs and behave as bosons of mass $2m_n$. They can then make a BEC through the BCS/BEC crossover mechanism. Therefore, neutron stars could actually be BEC stars. Since the maximum mass of BEC stars $M^a_{\rm max} = 0.0612\sqrt{\lambda}M_P^3/m^2 = 0.307\hbar c^2\sqrt{a}/(Gm)^{3/2}$ depends on the self-interaction constant λ (or scattering length a), it can be larger than the Oppenheimer-Volkoff limit $M_{OV} = 0.376M_P^3/m_n^2 = 0.7M_\odot$ obtained by assuming that neutron stars can be modeled as an ideal gas of fermions (the corresponding radius is $R = 9.36\,GM_{OV}/c^2 = 3.52(M_P/m_n)\lambda_c = 9.6\,\mathrm{km}$ and the corresponding

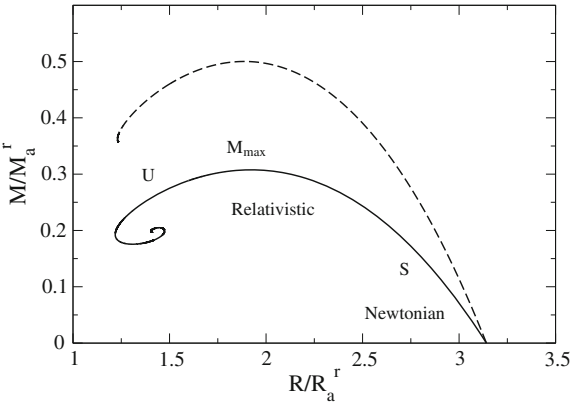

Fig. 6.6 Mass-radius relation of general relativistic BEC stars in the TF limit (*solid line* relativistic equation of state; *dashed line* non-relativistic equation of state). The series of equilibria is stable until the point of maximum mass

density is $\rho = 5 \times 10^{15}\,\mathrm{g\,cm^{-3}}$). By taking a scattering length of the order of 10–20 fm (hence $\lambda/8\pi \sim 95.2-190$), we obtain a maximum mass of the order of $2M_\odot$, a central density of the order of $1\text{–}3\times 10^{15}\,\mathrm{g\,cm^{-3}}$, and a radius in the range of 10–20 km [73]. This could account for the recently observed neutron stars with masses in the range of $2\text{–}2.4M_\odot$ larger than the Oppenheimer-Volkoff limit.

The general relativistic treatment of BEC stars by Chavanis and Harko [73] can also be applied straightforwardly to the description of condensate dark matter stars that may have formed in the primordial universe by Jeans instability. These compact objects should contain a significant fraction of condensate dark matter in their core and behave as BEC stars with the critical mass and radius given by Eqs. (6.84) and (6.85) above. When a condensate dark matter star is formed, it may accrete some material from space [91, 92]. The accretion process may increase the mass of the condensate star and, if the maximum mass is exceeded, cause the collapse of the condensate star. This collapse may form black holes from the dark matter star and have signature in the observations of high redshift long γ-ray bursts.

6.5.7 Are Microscopic Quantum Black Holes Bose-Einstein Condensates of Gravitons?

The Kaup mass (6.67), which is the maximum mass of a stable self-gravitating BEC resulting from the balance between quantum pressure (Heisenberg's uncertainty principle) and gravity in general relativity, scales as $M \sim M_P^2/m$. If N denotes the number of bosons in the BEC, so that $M = Nm$, we get $N \sim M_P^2/m^2$. On the other hand, the Kaup radius scales as $R \sim GM/c^2 \sim GM_P^2/mc^2 \sim \hbar/mc \sim \lambda_c \sim (M_P/m)l_P$ where $l_P = (\hbar G/c^3)^{1/2} = 1.62 \times 10^{-35}\,\mathrm{m}$ is the Planck length.

This corresponds to the "most packed" stable configuration. If we assume that the BEC remains stuck at the critical point, and if we take the number of bosons N as the sole characteristic of the BEC, the foregoing relations imply $m \sim M_P/\sqrt{N}$, $M \sim \sqrt{N}M_P$, and $R \sim \sqrt{N}l_P$. If we view microscopic quantum black holes as BECs of gravitons at a critical point, these scalings agree with those obtained by Dvali and Gomez [75] and Casadio and Orlandi [76] in a more phenomenological manner [the Gaussian profile obtained in [76] is also consistent with the Gaussian ansatz (6.44)]. In that interpretation, m is the effective mass of the gravitons and N is the occupation number of gravitons in the gravitational field, or the number of internal degrees of freedom of the black hole. For the gravitational interaction $-Gm^2/r$, the coupling constant scales as $\alpha \sim m^2/M_P^2 \sim l_P^2/\lambda_c^2 \sim 1/N$. We note that these scalings emerge naturally from the expression of the Kaup mass and Kaup radius, and N simply represents the number of bosons in the BEC. If we argue that the entropy of the "BEC black hole" scales as $S_{BH} \sim k_B N$ (originating from the exponentially growing with N number of quantum states [75]), we immediately recover the expression of the Bekenstein entropy $S_{BH} \sim k_B R^2/l_P^2$ stating that the entropy of a black hole scales as its area [93]. Finally, defining the temperature by the thermodynamical expression $d(Mc^2) = TdS_{BH}$, we obtain the scaling of the Hawking temperature $k_B T \sim mc^2 \sim M_P^2 c^2/M \sim \hbar c^3/GM \sim \hbar c/R \sim M_P c^2/\sqrt{N} \sim k_B T_P/\sqrt{N}$ where $T_P = (\hbar c^5/Gk_B^2)^{1/2} = 1.42 \times 10^{32}$ K is the Planck temperature. Inversely, if we define the temperature by $k_B T \sim mc^2$, we can derive from the first law of thermodynamics $d(Mc^2) = TdS_{BH}$ the black hole entropy $S_{BH} \sim N \sim k_B R^2/l_P^2$. In summary, we have the scalings

$$m \sim \frac{M_P}{\sqrt{N}}, \quad M \sim \sqrt{N}M_P, \quad R \sim \sqrt{N}l_P, \quad S \sim k_B N, \quad T \sim \frac{T_P}{\sqrt{N}}, \quad \alpha \sim \frac{1}{N}. \tag{6.86}$$

These scalings assume that the BEC remains stuck at the Kaup quantum critical point. As a result, the effective mass of the gravitons (that are massless) increases as N decreases (see below). We can also obtain the scalings (6.86) from the maximum mass (6.70) provided that the self-interaction constant scales as $\lambda \sim m^2/M_P^2 \sim 1/N$ (i.e. $a \sim \lambda\hbar/mc \sim Gm/c^2 \sim (m/M_P)l_P \sim l_P/\sqrt{N}$) which corresponds to the limit of validity of the TF approximation. We note that $a_S = 2Gm/c^2$ is the Schwarzschild radius of a particle of mass m.

As shown by Dvali and Gomez [75], the Hawking radiation[3] according to which black holes lose mass and energy, and the negative specific heat of the black holes[4] immediately result from the quantum depletion of the condensates by spontaneous

[3] In the semi-classical limit, the radiation of a black hole may be obtained from the Stefan-Boltzmann law $\dot{M}c^2 \sim -A\sigma T^4 \sim -\hbar c^6/G^2M^2$ where $\sigma \sim k_B^4/c^2\hbar^3$ is the black body constant and $A \sim R^2$ the black hole area. Using the scalings (6.86), this equation may be rewritten as $\dot{N} \sim -1/(t_P\sqrt{N})$ where $t_P = (\hbar G/c^5)^{1/2} = 5.39 \times 10^{-44}$ s is the Planck time. After integration, we obtain the scaling of the evaporation time of a black hole $\tau \sim M^3G^2/\hbar c^4 \sim N^{3/2}t_P$.

[4] Using $E \sim Mc^2 \sim \hbar c^5/Gk_B T$, we get $C = dE/dT \sim -\hbar c^5/Gk_B T^2 < 0$ so that the temperature increases as the black hole loses mass and energy.

particle emission. Actually, the arguments of Dvali and Gomez [75] generalize the semi-classical results of Hawking ($N \gg 1$) to the fully quantum regime (small N). We note that the mass $M \sim \sqrt{N}M_P$ and the area $A \sim R^2 \sim Nl_P^2$ of a black hole are *quantized* since N (occupation number) is an integer [94]. Each transition reduces the horizon area of a black hole by an integer number of Planck units. For $N = 1$ (ground state), we get $R \sim l_P$, $M = m \sim M_P$, and $T \sim T_P$ leading to Planck-size black holes (the Schwarzschild radius $a_S = 2Gm/c^2$ is of the order of the gravitational Bohr radius $a_B = \hbar^2/Gm^3$) [76] . These smallest black holes, instead of conventional Hawking evaporation [85, 95], are either stable (similarly to the $n = 1$ orbit of an electron around a proton whose stability is explained by quantum mechanics) or decay into the light fields in a single quantum jump. The classical limit is recovered for $N \gg 1$. Quantization of the horizons, and the notion of a minimal length in gravity, may eliminate physical singularities in cosmology (big bang and big crunch) [96]. Classical singularities may be replaced by a Planck black hole (with mass M_P and size l_P) and the scale factor $a(t)$ of the universe may become quantized as we approach the Planck scale. We note that in order to describe the inflationary era, the early universe viewed as a primordial black hole must gain energy and grow instead of radiating energy and decay. We therefore require a reversed flux of energy.

6.6 Conclusion

In this contribution, we have discussed some applications of self-gravitating BECs in astrophysics and their possible relation to black holes. We have exposed their elementary properties in Newtonian gravity and general relativity. There are many topics related to self-gravitating BECs that we have not discussed. They concern for example their formation by Jeans instability [15, 23, 28, 30, 33, 97, 98], their rotation leading to quantum vortex lattices [45, 99–103], their solitonic behavior [104–106], their gravitational cooling through emission of scalar field radiation [60, 65, 107], and their application to cosmology [50, 108–119]. Furthermore, we have exclusively considered BECs at $T = 0$ but the case of finite temperature BECs is also important [116, 120–126]. We refer to [64, 68, 127–136] for additional reviews on the subject.

An important potential application of self-gravitating BECs concerns the superfluid core of neutron stars and the notion of BEC stars [73]. For these compact objects, general relativity must be used and leads to the existence of a maximum mass $M_{\rm max} = 0.0612\sqrt{\lambda}M_P^3/m^2 = 0.307\hbar c^2\sqrt{a}/(Gm)^{3/2}$ above which no equilibrium is possible. For $M < M_{\rm max}$, stable BEC stars may describe neutron stars with a mass larger than the Oppenheimer-Volkoff limit [73]. For $M > M_{\rm max}$, the BECs should collapse and form stellar mass black holes. The formation of supermassive black holes is also possible if the BECs have negative scattering lengths corresponding to attractive short-range interactions. Again, there exist a maximum mass $M_{\rm max} = 1.012\hbar/\sqrt{|a|Gm} = 5.07M_P/\sqrt{|\lambda|}$ (usually very small) above which the BECs collapse [15]. On the other hand, stable BEC stars with a small (repulsive)

self-interaction may mimic supermassive black holes that reside at the center of galaxies [67, 69, 72]. Finally, the recent idea that black holes are BECs of gravitons stuck at a critical point [75] is fascinating.

Another application of self-gravitating BECs concerns dark matter halos. For these gigantic diluted objects, the Newtonian approximation can be used. In that context, the interest of the BEC model is to avoid the cusp problem and the missing satellite problem of the ΛCDM model. Indeed, gravitational collapse is prevented at small scales by the Heisenberg uncertainty principle or by repulsive short-range interactions. However, this scenario also encounters some problems. In the non-interacting case, the mass of the bosons must be extremely small, of the order of $m \sim 10^{-24}\,\mathrm{eV}/c^2$, in order to reproduce the properties of dark matter halos [17]. The existence of particles with such small masses is not established (but it is not ruled out neither). On the other hand, for self-interacting BECs in the TF approximation, the radius of the halo turns out to be independent on the total mass, and fixed by the properties of the bosons (their mass and scattering length) [40]. This is a major drawback of the BEC model because it implies that all the halos should have the same radius (unless the characteristics of the bosons change from halo to halo), which is clearly not the case. Going beyond the TF approximation does not help because it is found [15, 16] that the size of the self-gravitating BECs decreases with their mass while cosmological observations reveal that the size of the halos increases with the mass. It is possible that the BEC model at $T = 0$ describes only small halos (dwarf galaxies). In order to describe large halos, finite temperature effects should be taken into account. Finite temperature effects in the self-gravitating Bose gas have been studied in [120–122, 125]. In that case, the system has a core-halo structure with a small condensed core (equivalent to a BEC at $T = 0$) surrounded by an extended isothermal classical atmosphere of non-condensed bosons.

Another possible scenario is that dark matter is made of fermions (such as massive neutrinos) instead of bosons. This model also solves the cusp problem and the missing satellite problem. In that case, gravitational collapse is prevented at small scales by the Pauli exclusion principle. As for bosons, it may be necessary to consider the Fermi gas at finite temperature that displays interesting phase transitions between gaseous states and condensed states [137]. Originally, the self-gravitating Fermi gas at finite temperature with neutrino masses in the $\sim\ \mathrm{eV}/c^2$ range was proposed as a model for dark matter halos (e.g. $M = 10^{12}M_\odot$ and $R = 100\,\mathrm{kpc}$) and clusters of galaxies [138–140]. Then, it was suggested that degenerate superstars composed of weakly interacting fermions in the $\sim 10\,\mathrm{keV}/c^2$ range could be an alternative to the supermassive black holes that are reported to exist at the centers of galaxies (e.g. $M = 2.6 \times 10^6 M_\odot$ and $R = 18\,\mathrm{mpc}$ in our Galaxy) [141–143]. Finally, it was shown that a weakly interacting fermionic gas at finite temperature could provide a self-consistent model of dark matter that describes both the center and the halo of the galaxies [144]. Since the density of a self-gravitating isothermal sphere decreases as r^{-2} at large distances, this model is consistent with the flat rotation curves of the galaxies. On the other hand, since the core is degenerate in the sense of quantum

mechanics (Pauli exclusion principle), it leads to flat density profiles and avoids the cusp problem of cold dark matter models. In addition, the gravitational collapse of fermionic matter leads to a compact object (fermion ball) at the center of the galaxy that could be an alternative to a central black hole.

One difficulty with the finite temperature self-gravitating Bose and Fermi gases is to explain how the particles have thermalized and reached a statistical equilibrium state. Indeed, the relaxation time of self-gravitating systems is usually very large, exceeding the age of the universe by many orders of magnitude [1]. To solve this timescale problem, we have proposed [15] that dark matter should be considered as a collisionless system (made either of fermions or bosons) described by the Vlasov-Poisson system and undergoing a form of violent relaxation. This process, initially introduced by Lynden-Bell [145] in stellar dynamics, leads to a distribution function similar to the Fermi-Dirac distribution function. In that case, the origin of the "degeneracy" is due to dynamical constraints (Liouville's theorem) instead of quantum mechanics (Pauli's principle). This theory was initially developed to describe collisionless stellar systems such as elliptical galaxies. In that case, the non-degenerate limit may be the most relevant [145]. However, this approach (with dynamical degeneracy retained) could also apply to dark matter halos [146, 147]. In that case, gravitational collapse is prevented by Lynden-Bell's type of exclusion principle. Furthermore, this approach provides a much more efficient relaxation mechanism than the fermionic scenario. Indeed, the violent relaxation of collisionless systems (leading to the Lynden-Bell statistics) takes place on a few dynamical times while the collisional relaxation of fermions (leading to the Fermi-Dirac statistics) is very long and possibly unrealistic. Therefore, it is not clear how the fermions have thermalized and how they can possess sufficiently high temperatures. By contrast, the Lynden-Bell theory predicts a high effective temperature (even if $T = 0$ initially), a r^{-2} density profile at large distances consistent with the flat rotation curves of galaxies, and an effective exclusion principle at short distances that could avoid the cusp problem and lead to fermion balls mimicking black holes, just as in the fermionic scenario. These features are remarkably consistent with the observations of dark matter halos making this alternative scenario very attractive.

In the fermionic and bosonic models, the smooth core density of dark matter halos is justified by quantum mechanics. However, we would like to emphasize that a classical self-gravitating isothermal gas (possibly justified by the process of violent relaxation) also has a smooth core density due to finite temperature effects [148]. Therefore, classical isothermal, or almost isothermal, self-gravitating systems may be the most relevant description of large dark matter halos while quantum effects (for bosons or fermions) or Lynden-Bell's type of degeneracy (for collisionless systems) may be important only for small halos or in the very inner region of large halos. These promising ideas will be developed in future works.

Appendix

6.7 Self-interaction Constant

We define the self-interaction constant by [15]:

$$\frac{\lambda}{8\pi} \equiv \frac{a}{\lambda_c} = \frac{amc}{\hbar}, \tag{6.87}$$

where $\lambda_c = \hbar/mc$ is the Compton wavelength of the bosons. This is a dimensionless parameter measuring the strength of the short-range interactions. It can be written as

$$\frac{\lambda}{8\pi} = 5.07\, \frac{a}{1\,\text{fm}}\, \frac{m}{1\,\text{GeV}/c^2}. \tag{6.88}$$

Using this expression, we can express the results in terms of λ and m instead of a and m.

6.8 Conservation of Energy

The total energy associated with the quantum Euler-Poisson system (6.14)–(6.16) is given by Eq. (6.37). According to Eq. (6.38), we have

$$\delta\Theta_c = \int \frac{\mathbf{u}^2}{2}\delta\rho\, d\mathbf{r} + \int \rho\mathbf{u}\cdot\delta\mathbf{u}\, d\mathbf{r}. \tag{6.89}$$

On the other hand, using Eqs. (6.10) and (6.39), we find that

$$\begin{aligned}\delta\Theta_Q &= \frac{\hbar^2}{m^2}\int \nabla\sqrt{\rho}\cdot\delta\nabla\sqrt{\rho}\, d\mathbf{r} = \frac{\hbar^2}{m^2}\int \nabla\sqrt{\rho}\cdot\nabla\left(\frac{1}{2\sqrt{\rho}}\delta\rho\right) d\mathbf{r}\\ &= -\frac{\hbar^2}{2m^2}\int \frac{\Delta\sqrt{\rho}}{\sqrt{\rho}}\delta\rho\, d\mathbf{r} = \frac{1}{m}\int Q\delta\rho\, d\mathbf{r}.\end{aligned} \tag{6.90}$$

Finally, according to Eqs. (6.40) and (6.41), we have

$$\delta U = \frac{4\pi a\hbar^2}{m^3}\int \rho\delta\rho\, d\mathbf{r}, \quad \delta W = \int \Phi\delta\rho\, d\mathbf{r}. \tag{6.91}$$

Taking the time derivative of the total energy E_{tot} and using the previous relations, we get

$$\dot{E}_{tot} = \int\left(\frac{\mathbf{u}^2}{2} + \frac{Q}{m} + \frac{4\pi a\hbar^2}{m^3}\rho + \Phi\right)\frac{\partial\rho}{\partial t}\, d\mathbf{r} + \int \rho\mathbf{u}\cdot\frac{\partial\mathbf{u}}{\partial t}\, d\mathbf{r}. \tag{6.92}$$

Using the equation of continuity (6.14), integrating by parts, using the Euler equation (6.15) and the identity $(\mathbf{u}\cdot\nabla)\mathbf{u} = \nabla\left(\mathbf{u}^2/2\right) - \mathbf{u}\times(\nabla\times\mathbf{u})$, we obtain after simplification

$$\dot{E}_{tot} = \int \rho\mathbf{u}\cdot(\mathbf{u}\times(\nabla\times\mathbf{u}))\, d\mathbf{r}. \tag{6.93}$$

Since $\mathbf{u}$ is a potential flow, we have $\nabla\times\mathbf{u} = \mathbf{0}$ yielding $\dot{E}_{tot} = 0$. Actually, we note that this result remains valid even if $\mathbf{u}$ is not a potential flow since $\mathbf{u}\cdot(\mathbf{u}\times(\nabla\times\mathbf{u})) = 0$.

6.9 Virial Theorem

In this Appendix, we establish the time-dependent tensorial Virial theorem associated with the quantum Euler-Poisson system (6.14)–(6.16).

Taking the time derivative of the moment of inertia tensor $I_{ij} = \int \rho x_i x_j\, d\mathbf{r}$ and using the equation of continuity (6.14), we obtain after an integration by parts

$$\dot{I}_{ij} = \int \rho(x_i u_j + x_j u_i)\, d\mathbf{r}. \tag{6.94}$$

Taking the time derivative of Eq. (6.94), we get

$$\ddot{I}_{ij} = \int x_i \frac{\partial}{\partial t}(\rho u_j)\, d\mathbf{r} + (i\leftrightarrow j), \tag{6.95}$$

where $\partial_t(\rho u_j)$ is given by Eq. (6.13). We need to evaluate four terms. The first term is

$$-\int x_i \partial_k(\rho u_j u_k)\, d\mathbf{r} = \int \rho u_i u_j\, d\mathbf{r}. \tag{6.96}$$

The second term is

$$-\int x_i \frac{\partial p}{\partial x_j}\, d\mathbf{r} = \delta_{ij}\int p\, d\mathbf{r}. \tag{6.97}$$

The third term is

$$-\int \rho x_i \frac{\partial \Phi}{\partial x_j}\, d\mathbf{r} = W_{ij}, \tag{6.98}$$

where W_{ij} is the potential energy tensor. It is a simple matter to show that this tensor is symmetric: $W_{ij} = W_{ji}$ [1]. The fourth term is

$$-\int x_i \frac{\rho}{m}\frac{\partial Q}{\partial x_j}\, d\mathbf{r} = -\int x_i \partial_k P_{jk}\, d\mathbf{r} = \int P_{ij}\, d\mathbf{r}, \tag{6.99}$$

where P_{ij} is the quantum pressure tensor defined by Eq. (6.17). Substituting these results in Eq. (6.95), we obtain the tensorial Virial theorem

$$\frac{1}{2}\ddot{I}_{ij} = \int \rho u_i u_j \, d\mathbf{r} + \int P_{ij} \, d\mathbf{r} + \delta_{ij} \int p \, d\mathbf{r} + W_{ij}. \tag{6.100}$$

Contracting the indices and using the fact that $\int P_{ii} \, d\mathbf{r} = 2\Theta_Q$ [this can be obtained from Eqs. (6.17) and (6.39)] and $W_{ii} = -\int \rho \mathbf{r} \cdot \nabla \Phi \, d\mathbf{r} = W$ [the Virial of the gravitational force in $d = 3$ is equal to the potential energy [1]], we obtain

$$\frac{1}{2}\ddot{I} = 2(\Theta_c + \Theta_Q) + 3 \int p \, d\mathbf{r} + W, \tag{6.101}$$

where $I = \int \rho r^2 \, d\mathbf{r}$ is the moment of inertia. For a steady state ($\ddot{I}_{ij} = 0$ and $\mathbf{u} = \mathbf{0}$), we obtain the equilibrium tensorial Virial theorem

$$\int P_{ij} \, d\mathbf{r} + \delta_{ij} \int p \, d\mathbf{r} + W_{ij} = 0 \tag{6.102}$$

and the scalar Virial theorem

$$2\Theta_Q + 3 \int p \, d\mathbf{r} + W = 0. \tag{6.103}$$

These results are valid for an arbitrary equation of state $p(\rho)$. For the equation of state (6.12), using $\int p \, d\mathbf{r} = U$, Eqs. (6.101) and (6.103) reduce to Eqs. (6.42) and (6.43).

6.10 Stress Tensor

The equation of continuity (6.14) may be written as

$$\frac{\partial \rho}{\partial t} + \nabla \cdot \mathbf{j} = 0, \tag{6.104}$$

where $\mathbf{j} = \rho \mathbf{u}$ is the density current. Using Eqs. (6.6) and (6.7), the density current can be expressed in terms of the wave function as

$$\mathbf{j} = \frac{N\hbar}{2i} \left(\psi^* \nabla \psi - \psi \nabla \psi^* \right). \tag{6.105}$$

On the other hand, the quantum Euler equation (6.13) may be written as

$$\frac{\partial \mathbf{j}}{\partial t} = -\nabla(\rho \mathbf{u} \otimes \mathbf{u}) - \nabla p - \rho \nabla \Phi - \frac{\rho}{m} \nabla Q. \tag{6.106}$$

Introducing the quantum pressure tensor, we find that the equation for the density current is given by

$$\frac{\partial j_i}{\partial t} = -\partial_j T_{ij} - \rho \partial_i \Phi, \tag{6.107}$$

where

$$T_{ij} = \rho u_i u_j + p\delta_{ij} + P_{ij} \tag{6.108}$$

is the stress tensor. Using Eq. (6.17), we have

$$T_{ij} = \rho u_i u_j + p\delta_{ij} - \frac{\hbar^2}{4m^2}\rho \partial_i \partial_j \ln \rho \tag{6.109}$$

or, alternatively,

$$T_{ij} = \rho u_i u_j + \left(p - \frac{\hbar^2}{4m^2}\Delta\rho\right)\delta_{ij} + \frac{\hbar^2}{4m^2}\frac{1}{\rho}\partial_i\rho\partial_j\rho. \tag{6.110}$$

Using Eqs. (6.6) and (6.7), we find after straightforward algebra that

$$\frac{\hbar^2}{4m^2}\frac{1}{\rho}\partial_i\rho\partial_j\rho = \frac{N\hbar^2}{4m}\frac{1}{|\psi|^2}(\psi^*\partial_i\psi + \psi\partial_i\psi^*)(\psi^*\partial_j\psi + \psi\partial_j\psi^*) \tag{6.111}$$

and

$$\rho u_i u_j = -\frac{N\hbar^2}{4m}\frac{1}{|\psi|^2}(\psi^*\partial_i\psi - \psi\partial_i\psi^*)(\psi^*\partial_j\psi - \psi\partial_j\psi^*). \tag{6.112}$$

Therefore

$$\rho u_i u_j + \frac{\hbar^2}{4m^2}\frac{1}{\rho}\partial_i\rho\partial_j\rho = \frac{N\hbar^2}{m}\mathrm{Re}\left(\frac{\partial\psi}{\partial x_i}\frac{\partial\psi^*}{\partial x_j}\right). \tag{6.113}$$

Regrouping these results, the stress tensor can be expressed in terms of the wave function as

$$T_{ij} = \frac{N\hbar^2}{m}\mathrm{Re}\left(\frac{\partial\psi}{\partial x_i}\frac{\partial\psi^*}{\partial x_j}\right) + \left(\frac{2\pi a\hbar^2}{m}N^2|\psi|^4 - \frac{N\hbar^2}{4m}\Delta|\psi|^2\right)\delta_{ij}. \tag{6.114}$$

Finally, we introduce the density of energy

$$e = \frac{\mathbf{u}^2}{2} + \frac{Q}{m} + \frac{2\pi a\hbar^2}{m^3}\rho + \frac{\Phi}{2}. \tag{6.115}$$

Using the equation of continuity (6.14) and the quantum Euler equation (6.15), we obtain the energy equation

$$\frac{\partial}{\partial t}(\rho e) + \nabla \cdot (\rho e \mathbf{u}) = -\nabla \cdot (p\mathbf{u}) - \frac{1}{2}\rho \mathbf{u} \cdot \nabla \Phi + \frac{\rho}{m}\frac{\partial Q}{\partial t} + \frac{1}{2}\rho \frac{\partial \Phi}{\partial t}. \tag{6.116}$$

The conservation of energy directly results from this equation. Taking the time derivative of the total energy $E_{tot} = \int \rho e \, d\mathbf{r}$, and using Eq. (6.116), we get

$$\dot{E}_{tot} = -\frac{1}{2}\int \rho \mathbf{u} \cdot \nabla \Phi \, d\mathbf{r} + \int \frac{\rho}{m}\frac{\partial Q}{\partial t} \, d\mathbf{r} + \frac{1}{2}\int \rho \frac{\partial \Phi}{\partial t} \, d\mathbf{r}. \tag{6.117}$$

Using the Poisson equation (6.16) and the equation of continuity (6.14), and integrating by parts, we obtain

$$\begin{aligned} \frac{1}{2}\int \rho \frac{\partial \Phi}{\partial t} \, d\mathbf{r} &= \frac{1}{8\pi G}\int \Delta \Phi \frac{\partial \Phi}{\partial t} \, d\mathbf{r} = \frac{1}{2}\int \Phi \frac{\partial \rho}{\partial t} \, d\mathbf{r} \\ &= -\frac{1}{2}\int \Phi \nabla \cdot (\rho \mathbf{u}) \, d\mathbf{r} = \frac{1}{2}\int \rho \mathbf{u} \cdot \nabla \Phi \, d\mathbf{r}. \end{aligned} \tag{6.118}$$

On the other hand, using Eqs. (6.38) and (6.90), we find that

$$\int \rho \frac{\partial Q}{\partial t} \, d\mathbf{r} = m\frac{d\Theta_Q}{dt} - \int Q \frac{\partial \rho}{\partial t} \, d\mathbf{r} = \int Q \frac{\partial \rho}{\partial t} \, d\mathbf{r} - \int Q \frac{\partial \rho}{\partial t} \, d\mathbf{r} = 0. \tag{6.119}$$

Substituting these identities in Eq. (6.117), we obtain $\dot{E}_{tot} = 0$.

6.11 Lagrangian and Hamiltonian

In this Appendix, we discuss the Lagrangian and Hamiltonian structure of the GP equation and of the corresponding hydrodynamic equations.

The Lagrangian of the GP equation (6.4) is

$$L = \int \left\{ i\frac{\hbar}{2}N\left(\psi^* \frac{\partial \psi}{\partial t} - \psi \frac{\partial \psi^*}{\partial t}\right) - \frac{N\hbar^2}{2m}|\nabla \psi|^2 - \frac{1}{2}Nm|\psi|^2 \Phi - \frac{2\pi a \hbar^2}{m}N^2|\psi|^4 \right\} d\mathbf{r}. \tag{6.120}$$

We can view the Lagrangian (6.120) as a functional of ψ, $\dot{\psi}$, and $\nabla\psi$. The action is $S = \int L \, dt$. The least action principle $\delta S = 0$, which is equivalent to the Lagrange equations

$$\frac{\partial}{\partial t}\left(\frac{\delta L}{\delta \dot{\psi}}\right) + \nabla \cdot \left(\frac{\delta L}{\delta \nabla \psi}\right) - \frac{\delta L}{\delta \psi} = 0 \tag{6.121}$$

returns the GP equation (6.4). The Hamiltonian is obtained from the transformation

$$H=\int i\frac{\hbar}{2}N\left(\psi^*\frac{\partial\psi}{\partial t}-\psi\frac{\partial\psi^*}{\partial t}\right)d\mathbf{r}-L \tag{6.122}$$

leading to

$$H=\int\left\{\frac{N\hbar^2}{2m}|\nabla\psi|^2+\frac{1}{2}Nm|\psi|^2\Phi+\frac{2\pi a\hbar^2}{m}N^2|\psi|^4\right\}d\mathbf{r}. \tag{6.123}$$

Of course, this expression coincides with the total energy (6.37) in the wavefunction representation. Using the Lagrange equations, one can show that the Hamiltonian is conserved. On the other hand, the GP equation (6.4) can be written as

$$i\hbar\frac{\partial\psi}{\partial t}=\frac{1}{N}\frac{\delta H}{\delta\psi^*}. \tag{6.124}$$

A stable stationary solution of the GP equation is a minimum of energy under the normalization condition. Writing the variational principle as $\delta H-\alpha Nm\int|\psi|^2\,d\mathbf{r}=0$ where α is a Lagrange multiplier (chemical potential), we recover the time-independent GP equation (6.19) with $E=\alpha m$.

Using the Madelung transformation (see Sect. 6.2.2), we can rewrite the Lagrangian and the Hamiltonian in terms of hydrodynamic variables. According to Eqs. (6.6) and (6.7) we have

$$\frac{\partial S}{\partial t}=\frac{\hbar}{2i}\frac{1}{|\psi|^2}\left(\psi^*\frac{\partial\psi}{\partial t}-\psi\frac{\partial\psi^*}{\partial t}\right) \tag{6.125}$$

and

$$|\nabla\psi|^2=\frac{1}{Nm\hbar^2}\left[\rho(\nabla S)^2+\frac{\hbar^2}{4\rho}(\nabla\rho)^2\right]. \tag{6.126}$$

Substituting these identities in Eq. (6.120) we get

$$L=-\int\left\{\frac{\rho}{m}\frac{\partial S}{\partial t}+\frac{\rho}{2m^2}(\nabla S)^2+\frac{\hbar^2}{8m^2}\frac{(\nabla\rho)^2}{\rho}+\frac{1}{2}\rho\Phi+\frac{2\pi a\hbar^2}{m^3}\rho^2\right\}d\mathbf{r}. \tag{6.127}$$

We can view the Lagrangian (6.127) as a functional of S, $\dot{S}$, ∇S, ρ, $\dot{\rho}$, and $\nabla\rho$. The Lagrange equations for the phase

$$\frac{\partial}{\partial t}\left(\frac{\delta L}{\delta\dot{S}}\right)+\nabla\cdot\left(\frac{\delta L}{\delta\nabla S}\right)-\frac{\delta L}{\delta S}=0 \tag{6.128}$$

return the equation of continuity (6.8). The Lagrange equations for the density

$$\frac{\partial}{\partial t}\left(\frac{\delta L}{\delta \dot{\rho}}\right)+\nabla\cdot\left(\frac{\delta L}{\delta \nabla\rho}\right)-\frac{\delta L}{\delta\rho}=0 \tag{6.129}$$

return the quantum Hamilton-Jacobi (or Bernouilli) equation (6.9) leading to the quantum Euler equation (6.15). The Hamiltonian is obtained from the transformation

$$H=-\int\frac{\rho}{m}\frac{\partial S}{\partial t}\,d\mathbf{r}-L \tag{6.130}$$

leading to

$$H=\int\left\{\frac{1}{2}\rho\mathbf{u}^2+\frac{\hbar^2}{8m^2}\frac{(\nabla\rho)^2}{\rho}+\frac{1}{2}\rho\Phi+\frac{2\pi a\hbar^2}{m^3}\rho^2\right\}d\mathbf{r}. \tag{6.131}$$

Of course, this expression coincides with the total energy (6.37) in the hydrodynamical representation. Using the Lagrange equations, one can show that the Hamiltonian is conserved.

References

1. Binney, J., Tremaine, S.: Galactic Dynamics. Princeton University Press, Princeton (1987)
2. Copeland, E.J., Sami, M., Tsujikawa, S.: Int. J. Mod. Phys. D **15**, 1753 (2006)
3. Persic, M., Salucci, P., Stel, F.: Mon. Not. R. Astron. Soc. **281**, 27 (1996)
4. Overduin, J.M., Wesson, P.S.: Phys. Rep. **402**, 267 (2004)
5. Peebles, P.J.E., Ratra, B.: Rev. Mod. Phys. **75**, 559 (2003)
6. Navarro, J.F., Frenk, C.S., White, S.D.M.: Mon. Not. R. Astron. Soc. **462**, 563 (1996)
7. Burkert, A.: Astrophys. J. **447**, L25 (1995)
8. Kauffmann, G., White, S.D.M., Guiderdoni, B.: Mon. Not. R. Astron. Soc. **264**, 201 (1993)
9. Pethick, C.J., Smith, H.: Bose-Einstein Condensation in Dilute Gases. Cambridge University Press, Cambridge (2008)
10. Madelung, E.: Zeit. F. Phys. **40**, 322 (1927)
11. Gross, E.P.: Ann. Phys. **4**, 57 (1958)
12. Gross, E.P.: Nuovo Cimento **20**, 454 (1961)
13. Gross, E.P.: J. Math. Phys. **4**, 195 (1963)
14. Pitaevskii, L.P.: Sov. Phys. JETP **9**, 830 (1959); ibid 13, 451 (1961)
15. Chavanis, P.H.: Phys. Rev. D **84**, 043531 (2011)
16. Chavanis, P.H., Delfini, L.: Phys. Rev. D **84**, 043532 (2011)
17. Baldeschi, M.R., Gelmini, G.B., Ruffini, R.: Phys. Lett. B **122**, 221 (1983)
18. Membrado, M., Pacheco, A.F., Sanudo, J.: Phys. Rev. A **39**, 4207 (1989)
19. Sin, S.J.: Phys. Rev. D **50**, 3650 (1994)
20. Schunck, F.E.: astro-ph/9802258
21. Matos, T., Guzmán, F.S.: Astron. F. Nachr. **320**, 97 (1999)
22. Guzmán, F.S., Matos, T.: Class. Quantum Gravity **17**, L9 (2000)
23. Hu, W., Barkana, R., Gruzinov, A.: Phys. Rev. Lett. **85**, 1158 (2000)
24. Matos, T., Ureña-López, L.A.: Phys. Rev. D **63**, 063506 (2001)
25. Arbey, A., Lesgourgues, J., Salati, P.: Phys. Rev. D **64**, 123528 (2001)

26. Silverman, M.P., Mallett, R.L.: Class. Quantum Gravity **18**, L103 (2001)
27. Alcubierre, M., Guzmán, F.S., Matos, T., Núñez, D., Ureña-López, L.A., Wiederhold, P.: Class. Quantum. Gravity **19**, 5017 (2002)
28. Silverman, M.P., Mallett, R.L.: Gen. Relativ. Gravit. **34**, 633 (2002)
29. Bernal, A., Matos, T., Núñez, D.: Rev. Mex. Astron. Astrofis. **44**, 149 (2008)
30. Sikivie, P., Yang, Q.: Phys. Rev. Lett. **103**, 111301 (2009)
31. Matos, T., Vazquez-Gonzalez, A., Magana, J.: Mon. Not. R. Astron. Soc. **393**, 1359 (2009)
32. Lee, J.W.: Phys. Lett. B **681**, 118 (2009)
33. Lee, J.W., Lim, S.: J. Cosmol. Astropart. Phys. **01**, 007 (2010)
34. Manfredi, G., Hervieux, P.A., Haas, F.: Class. Quantum Gravity **30**, 075006 (2013)
35. Lee, J.W., Koh, I.: Phys. Rev. D **53**, 2236 (1996)
36. Peebles, P.J.E.: Astrophys. J. **534**, L127 (2000)
37. Goodman, J.: New Astron. **5**, 103 (2000)
38. Lesgourgues, J., Arbey, A., Salati, P.: New Astron. Rev. **46**, 791 (2002)
39. Arbey, A., Lesgourgues, J., Salati, P.: Phys. Rev. D **68**, 023511 (2003)
40. Böhmer, C.G., Harko, T.: J. Cosmol. Astropart. Phys. **06**, 025 (2007)
41. Briscese, F.: Phys. Lett. B **696**, 315 (2011)
42. Harko, T.: J. Cosmol. Astropart. Phys. **05**, 022 (2011)
43. Pires, M.O.C., de Souza, J.C.C.: J. Cosmol. Astropart. Phys. **11**, 024 (2012)
44. Robles, V.H., Matos, T.: Mon. Not. R. Astron. Soc. **422**, 282 (2012)
45. Rindler-Daller, T., Shapiro, P.R.: Mon. Not. R. Astron. Soc. **422**, 135 (2012)
46. Lora, V., Magaña, J., Bernal, A., Sánchez-Salcedo, F.J., Grebel, E.K.: J. Cosmol. Astropart. Phys. **02**, 011 (2012)
47. González-Morales, A.X., Diez-Tejedor, A., Ureña-López, L.A., Valenzuela, O.: Phys. Rev. D **87**, 021301(R) (2013)
48. Guzmán, F.S., Lora-Clavijo, F.D., González-Avilés, J.J., Rivera-Paleo, F.J.: J. Cosmol. Astropart. Phys. **09**, 034 (2013)
49. Dalfovo, F., Giorgini, S., Pitaevskii, L.P., Stringari, S.: Rev. Mod. Phys. **71**, 463 (1999)
50. Chavanis, P.H.: Astron. Astrophys. **537**, A127 (2012)
51. Kaup, D.J.: Phys. Rev. **172**, 1331 (1968)
52. Ruffini, R., Bonazzola, S.: Phys. Rev. **187**, 1767 (1969)
53. Thirring, W.: Phys. Lett. B **127**, 27 (1983)
54. Breit, J.D., Gupta, S., Zaks, A.: Phys. Lett. B **140**, 329 (1984)
55. Takasugi, E., Yoshimura, M.: Z. Phys. C **26**, 241 (1984)
56. Colpi, M., Shapiro, S.L., Wasserman, I.: Phys. Rev. Lett. **57**, 2485 (1986)
57. van der Bij, J.J., Gleiser, M.: Phys. Lett. B **194**, 482 (1987)
58. Gleiser, M.: Phys. Rev. D **38**, 2376 (1988)
59. Gleiser, M., Watkins, R.: Nucl. Phys. B **319**, 733 (1989)
60. Seidel, E., Suen, W.M.: Phys. Rev. D **42**, 384 (1990)
61. Kusmartsev, F.V., Mielke, E.W., Schunck, F.E.: Phys. Lett. A **157**, 465 (1991)
62. Kusmartsev, F.V., Mielke, E.W., Schunck, F.E.: Phys. Rev. D **43**, 3895 (1991)
63. Lee, T.D., Pang, Y.: Phys. Rep. **221**, 251 (1992)
64. Jetzer, P.: Phys. Rep. **220**, 163 (1992)
65. Seidel, E., Suen, W.M.: Phys. Rev. Lett. **72**, 2516 (1994)
66. Balakrishna, J., Seidel, E., Suen, W.M.: Phys. Rev. D **58**, 104004 (1998)
67. Schunck, F.E., Liddle, A.R.: Black holes: theory and observation. In: Hehl, F.W., Kiefer, C., Metzler, R.J.K. (eds.) Proceedings of the 179th W.E. Heraeus Seminar, p. 285. Springer (1998)
68. Mielke, E.W., Schunck, F.E.: Nucl. Phys. B **564**, 185 (2000)
69. Torres, D.F., Capozziello, S., Lambiase, G.: Phys. Rev. D **62**, 104012 (2000)
70. Wang, X.Z.: Phys. Rev. D **64**, 124009 (2001)
71. Schunck, F.E., Mielke, E.W.: Class. Quantum Gravity **20**, R301 (2003)
72. Guzmán, F.S.: Phys. Rev. D **73**, 021501 (2006)
73. Chavanis, P.H., Harko, T.: Phys. Rev. D **86**, 064011 (2012)

74. Oppenheimer, J.R., Volkoff, G.M.: Phys. Rev. **55**, 374 (1939)
75. Dvali, G., Gomez, C.: Fortschr. Phys. **61**, 742 (2013)
76. Casadio, R., Orlandi, A.: J. High Energy Phys. **8**, 25 (2013)
77. Bohm, D.: Phys. Rev. **85**, 166 (1952)
78. Chandrasekhar, S.: An Introduction to the Study of Stellar Structure. Dover, Mineola, New York (1958)
79. von Weizsäcker, C.F.: Z. Phys. **96**, 431 (1935)
80. Fisher, R.A.: Proc. Cambridge Philos. Soc. **22**, 700 (1925)
81. Holm, D., Marsden, J., Ratiu, T., Weinstein, A.: Phys. Rep. **123**, 1 (1985)
82. Chavanis, P.H.: Phys. Rev. E **84**, 031101 (2011)
83. Sulem, C., Sulem, P.L.: The Nonlinear Schrödinger Equation. Springer, Berlin (1999)
84. Ledoux, P., Pekeris, C.L.: Astrophys. J. **94**, 124 (1941)
85. Hawking, S.: Nature **248**, 30 (1974)
86. Lee, T.D.: Phys. Rev. D **35**, 3637 (1987)
87. Torres, D.F.: Nucl. Phys. B **26**, 377 (2002)
88. Misner, C.W., Zapolsky, H.S.: Phys. Rev. Lett. **12**, 635 (1964)
89. Harrison, B.K., Thorne, K.S., Wakano, M., Wheeler, J.A.: Gravitation Theory and Gravitational Collapse. University of Chicago Press, Chicago (1965)
90. Chavanis, P.H.: Astron. Astrophys. **381**, 709 (2002)
91. Li, X.Y., Harko, T., Cheng, K.S.: J. Cosmol. Astropart. Phys. **06**, 001 (2012)
92. Li, X.Y., Wang, F.Y., Cheng, K.S.: J. Cosmol. Astropart. Phys. **10**, 031 (2012)
93. Bekenstein, J.D.: Phys. Rev. D **7**, 2333 (1973)
94. Dvali, G., Gomez, C., Mukhanov, S.: arXiv:1106.5894
95. Hawking, S.: Commun. Math. Phys. **43**, 199 (1975)
96. Dvali, G., Gomez, C., Mukhanov, S.: J. High Energy Phys. **2**, 12 (2011)
97. Khlopov, M.Y., Malomed, B.A., Zeldovich, Y.B.: Mon. Not. R. Astron. Soc. **215**, 575 (1985)
98. Bianchi, M., Grasso, D., Ruffini, R.: Astron. Astrophys. **231**, 301 (1990)
99. Kobayashi, Y., Kasai, M., Futamase, T.: Phys. Rev. D **50**, 7721 (1994)
100. Yoshida, S., Eriguchi, Y.: Phys. Rev. D **56**, 762 (1997)
101. Schunck, F.E., Mielke, E.W.: Phys. Lett. A **249**, 389 (1998)
102. Kain, B., Ling, H.Y.: Phys. Rev. D **82**, 064042 (2010)
103. Guzmán, F.S., Lora-Clavijo, F.D., González-Avilés, J.J., Rivera-Paleo, F.J.: arXiv:1310.3909
104. Bernal, A., Guzmán, F.S.: Phys. Rev. D **74**, 103002 (2006)
105. Lee, J.W., Lim, S., Choi, D.: arXiv:0805.3827
106. González, J.A., Guzmán, F.S.: Phys. Rev. D **83**, 103513 (2011)
107. Guzmán, F.S., Ureña-López, L.A.: Phys. Rev. D **645**, 814 (2006)
108. Fukuyama, T., Morikawa, M., Tatekawa, T.: J. Cosmol. Astropart. Phys. **06**, 033 (2008)
109. Fukuyama, T., Morikawa, M.: Phys. Rev. D **80**, 063520 (2009)
110. Harko, T.: Mon. Not. R. Astron. Soc. **413**, 3095 (2011)
111. Chavanis, P.H.: Phys. Rev. D **84**, 063518 (2011)
112. Harko, T.: Phys. Rev. D **83**, 123515 (2011)
113. Bettoni, D., Liberati, S., Sindoni, L.: J. Cosmol. Astropart. Phys. **11**, 007 (2011)
114. Magaña, J., Matos, T., Suárez, A., Sánchez-Salcedo, F.J.: J. Cosmol. Astropart. Phys. **10**, 003 (2012)
115. Park, C.G., Hwang, J.C., Noh, H.: Phys. Rev. D **86**, 083535 (2012)
116. Harko, T., Mocanu, G.: Phys. Rev. D **85**, 084012 (2012)
117. Velten, H., Wamba, E.: Phys. Lett. B **709**, 1 (2012)
118. Kain, B., Ling, H.Y.: Phys. Rev. D **85**, 023527 (2012)
119. Li, B., Rindler-Daller, T., Shapiro, P.R.: arXiv:1310.6061
120. Ingrosso, G., Ruffini, R.: Nuovo Cimento **101**, 369 (1988)
121. Ingrosso, G., Merafina, M., Ruffini, R.: Nuovo Cimento **105**, 977 (1990)
122. Bilic, N., Nikolic, H.: Nucl. Phys. B **590**, 575 (2000)
123. Matos, T., Suárez, A.: Europhys. Lett. **96**, 56005 (2011)
124. Harko, T., Madarassy, E.: J. Cosmol. Astropart. Phys. **01**, 020 (2012)

125. Slepian, Z., Goodman, J.: Mon. Not. R. Astron. Soc. **427**, 839 (2012)
126. Robles, V.H., Matos, T.: Astrophys. J. **763**, 19 (2013)
127. Liddle, A.R., Madsen, M.S.: Int. J. Mod. Phys. D **1**, 101 (1992)
128. Guzmán, F.S.: J. Phys.: Conf. Series **91**, 012003 (2007)
129. Lee, J.W.: Korean Phys. Soc. **54**, 2622 (2009)
130. Liebling, S.L., Palenzuela, C.: Living Rev. Relativ. **15**, 6 (2012)
131. Magaña, J., Matos, T.: J. Phys.: Conf. Series **378**, 012012 (2012)
132. Magaña, J., Matos, T., Robles, V., Suárez, A.: arXiv:1201.6107
133. Rindler-Daller, T., Shapiro, P.R.: arXiv:1209.1835
134. Suárez, A., Robles, V.H., Matos, T.: arXiv:1302.0903
135. Dwornik, M., Keresztes, Z., Gergely L.A.: arXiv:1312.3715
136. Rindler-Daller, T., Shapiro, P.R.: Mod. Phys. Lett. A **29**, 1430002 (2014)
137. Chavanis, P.H.: Int. J. Mod. Phys. B **20**, 3113 (2006)
138. Fabbri, R., Jantzen, R., Ruffini, R.: Astron. Astrophys. **114**, 219 (1982)
139. Ruffini, R., Stella, L.: Astron. Astrophys. **119**, 35 (1983)
140. Gao, J.G., Merafina, M., Ruffini, R.: Astron. Astrophys. **235**, 1 (1990)
141. Bilic, N., Viollier, R.D.: Phys. Lett. B **408**, 75 (1997)
142. Bilic, N., Viollier, R.D.: Eur. Phys. J. C **11**, 173 (1999)
143. Bilic, N., Lindebaum, R.J., Tupper, G.B., Viollier, R.D.: Phys. Lett. B **515**, 105 (2001)
144. Bilic, N., Tupper, G.B., Viollier, R.D.: Lect. Notes Phys. **616**, 24 (2003)
145. Lynden-Bell, D.: Mon. Not. R. Astron. Soc. **136**, 101 (1967)
146. Kull, A., Treumann, R.A., Böhringer, H.: Astrophys. J. **466**, L1 (1996)
147. Chavanis, P.H., Sommeria, J.: Mon. Not. R. Astron. Soc. **296**, 569 (1998)
148. Chavanis, P.H.: Astron. Astrophys. **381**, 340 (2002)